

Phosphoproteomic analysis and protein-protein interaction of rat aorta GJA1 and rat heart FKBP1A after secoiridoids consumption from virgin olive oil: A functional proteomics approach.

Anna Pedret^{1, 2}, Úrsula Catalán^{1, 2, 3, *}, Laura Rubió^{1, 4}, Isabel Baiges⁵, Pol Herrero⁵, Carme Piñol^{6, 7}, Ricardo Rodríguez-Calvo^{3, 8, 9, 10}, Núria Canela⁵, Sara Fernández-Castillejo^{1, 2}, Maria-Jose Motilva¹¹, Rosa Solà^{1, 2, 10}

¹ Universitat Rovira i Virgili, Faculty of Medicine and Health Sciences, Medicine and Surgery Department, Functional Nutrition, Oxidation, and CVD Research Group (NFOC-Salut), Reus, Spain.

² Eurecat, Centre Tecnològic de Catalunya, Unitat de Nutrició i Salut, Reus, Spain.

³ Institut d'Investigació Sanitària Pere Virgili (IISPV), Reus, Spain.

⁴ Food Technology Department, Universitat de Lleida-AGROTECNIO Center, Lleida, Spain

⁵ Eurecat, Centre Tecnològic de Catalunya. Centre for Omic Sciences (COS), Joint Unit Universitat Rovira i Virgili-EURECAT. Reus, Spain

⁶ Department of Medicine, Universitat de Lleida, Lleida, Catalonia

⁷ Institut de Recerca Biomèdica de Lleida Fundació Dr. Pifarré-IRBLleida, Lleida, Spain

⁸ Universitat Rovira i Virgili, Research Unit on Lipids and Atherosclerosis, Vascular Medicine and Metabolism Unit, Reus, Spain.

⁹ Spanish Biomedical Research Centre in Diabetes and Associated Metabolic Disorders (CIBERDEM), Institute of Health Carlos III, Madrid, Spain.

¹⁰ Hospital Universitari Sant Joan de Reus (HUSJR), Reus, Spain.

¹¹ Instituto de Ciencias de la Vid y del Vino-ICVV CSIC, Gobierno de La Rioja, Universidad de La Rioja, Logroño, Spain.

*Corresponding author:

Úrsula CATALÁN, PhD

Tel: (+34) 977 75 93 77

Fax: (+34) 977 75 93 22

E-mail: ursula.catalan@eurecat.org

1 **Abstract:**

2 Protein functional interactions could explain the biological response of secoiridoids (SECs),
3 main phenolic compounds in virgin olive oil (VOO). The aim was to assess protein-protein
4 interactions (PPIs) of the aorta gap junction alpha-1 (GJA1) and the heart peptidyl-prolyl cis-
5 trans isomerase (FKBP1A), plus the phosphorylated heart proteome, to describe new molecular
6 pathways in the Cardiovascular System in rats using nanoliquid chromatography coupled with
7 mass-spectrometry. PPIs modified by SECs and associated with GJA1 in aorta rat tissue were
8 calpain, TUBA1A, and HSPB1. Those associated with FKBP1A in rat heart tissue included
9 SUCLG1, HSPE1, and TNNI3. In the heart, SECs modulated the phosphoproteome through the
10 main canonical pathways PI3K/mTOR signaling (AKT1S1, GAB2) and Gap Junction signaling
11 (GAB2, GJA1). PPIs associated with GJA1 and with FKBP1A, the phosphorylation of GAB2,
12 and the dephosphorylation of GJA1 and AKT1S1 in rat tissues are promising protein targets
13 promoting cardiovascular protection, to explain the health benefits of VOO.

14

15 **Keywords:** secoiridoids; protein-protein interactions; phosphoproteome; proteome; tissues

16

17

18

19

20

21

22

23

24 INTRODUCTION

25 Phenolic compounds are minor components of virgin olive oil (VOO) ¹, whereas hydroxytyrosol
26 (HT) is the major phenolic compound in VOO in both its free and complex forms: esterified
27 derivatives with elenolic acid called secoiridoids (SECs) ². During mechanical extraction of
28 VOO, hydrolysis reactions take place by endogenous β -glucosidases of the olive fruits,
29 releasing aglycone derivatives known as SECs. Chemically, SECs are characterized by the
30 presence of elenolic acid or some of its derivatives, and HT or tyrosol in their molecule ³. HT
31 and SECs present in VOO have shown a wide range of biological activities, such as antioxidant,
32 anticancer, and neuroprotective, also having cardiovascular beneficial effects ^{4,5}.

33 With the rising need to identify a new mechanism of action explaining the health benefits of
34 VOO, proteomics is a novel and promising tool ⁶. In this context, scarce data are available in
35 terms of investigating the possible protective effects of phenolic compounds in VOO in
36 cardiovascular tissues such as the aorta and/or heart.

37 In a previous study conducted by our group based on descriptive proteomics, we demonstrated
38 that the proteome is modulated after HT or SEC diet supplementation in the heart tissue and
39 aortic tissue of healthy rats ⁴. The study showed that there is a role for HT and SECs in the
40 regulation of proteins that are related to the proliferation and migration of endothelial cells and
41 the occlusion of blood vessels in aortic tissue and in the regulation of proteins related to heart
42 failure in heart tissue. Thus, in that study, SECs had higher fold change (FC) values compared
43 to HT, which was attributable to the higher concentration of HT biological metabolites detected
44 in rat heart tissue after an SEC diet ⁴. In a healthy rat model, SEC diet supplementation was
45 compared to a control diet, and it was observed that two proteins were modified throughout the
46 entire proteome of the cardiovascular system: connexin 43 (Cx43; nomenclature based on the
47 predicted molecular mass), also known as the gap junction alpha-1 protein (GJA1; nomenclature
48 based on the gene sequence), which was significantly downregulated in aortic tissue (-1.7 FC);
49 and FK506 Binding Protein 12 (FKBP12), also known as peptidyl-prolyl cis-trans isomerase
50 (FKBP1A), which was significantly upregulated in heart tissue (+1.7 FC) ⁴.

51 Cx43 is a large family of transmembrane proteins that are involved in the vascular remodeling
52 associated with atherosclerosis, which causes the exchange of ions and small metabolites
53 between the cytosol and extracellular space or between neighboring cells ⁷. During
54 atherosclerosis, Cx43 (GJA1) expression in intimal smooth muscle cells is sequentially
55 increased in the early atheroma stage ⁷. Additionally, GJA1 monocytic cell junctions are
56 significantly upregulated in patients with atherosclerosis, which is correlated with the
57 generation of gap and tight junctions that then have important roles in atherosclerosis ⁸.

58 FKBP1A is the predominant isoform associated with cardiac tissue in most mammals ⁹.
59 Unlike GJA1, the downregulation of FKBP1A is related to heart failure, hypertrophy of the left
60 ventricle, congestive heart failure, or systolic dysfunction in the heart. Consequently, FKBP1A
61 upregulation could have a positive effect, preventing abnormalities in the cardiac structure,
62 including a lack of compaction or thin ventricular walls ¹⁰.

63 Thus, considering what we observed in our previous study—the downregulation of the protein
64 expression of GJA1 and the upregulation of FKBP1A with SEC diet supplementation ⁴—the
65 specific biological functions and cellular-related mechanisms of these proteins need to be
66 elucidated. In addition to descriptive proteomics for heart and aortic tissues, functional
67 proteomics provides information on the conformation, modification, interaction, and subcellular
68 localization of proteins in a proteome-wide, unbiased, and high-throughput manner, revealing
69 biological functions and cellular mechanisms ¹¹. Emerging methods such as crosslinking mass
70 spectrometry and advanced protein correlation profiling will enable future in situ analyses of
71 mechanosensing in terms of protein interactions. The use of these mass spectrometry toolsets
72 combined with post-translational modification (PTM) analyses, such as phosphorylation, will
73 ultimately move the field toward being able to obtain a comprehensive list of molecular
74 alterations in cellular mechanosensing ¹². Therefore, protein–protein interactions (PPIs) and
75 phosphorylation, one of the main PTMs ¹³, will be key indicators of protein activity ¹³ at the
76 specific time point at which they are analyzed.

77 The main goal of this work was to go beyond traditional descriptive proteomics knowledge by
78 evaluating functional proteomics through an assessment of PPIs associated with GJA1 in rat
79 aortic tissue, PPIs associated with FKBP1A in rat heart tissue, and the phosphoproteomic profile
80 of rat heart tissue to elucidate how SECs are involved in cardiovascular disease prevention.

81 **MATERIALS AND METHODS**

82 *Animals and diets*

83 Eight female Wistar rats weighing 300–350 g were obtained from Charles River Laboratories
84 (Barcelona, Spain) and separated into two groups with different diets (four rats per group): the
85 control group (A) and the SEC group (B). The animal procedures were performed as in our
86 previous work ⁴ and were approved by the Animal Ethics Committee of the Universitat de
87 Lleida (CEEA 10-06/14, 31 July 2014).

88 For the SEC diet group, commercial feed pellets (Harlan Laboratories, Madison, WI, USA)
89 were crushed in an industrial mill and mixed with Milli-Q water containing the equivalent of 5
90 mg of SECs/kg rat weight in 16 g of crushed pellets (average daily consumption per rat). New
91 pellets were prepared and freeze-dried until use. The feed and animals were weighed every 2
92 days to adjust the weekly dose of the phenolic compounds to 5 mg/kg rat weight/day. The dose
93 administered was equivalent to a 0.81-mg/kg dose in humans, which equates to 48.6 mg for a
94 60-kg person, a dose achievable with phenol-rich olive oil.

95 After 21 days of diet supplementation, rats were sacrificed through an intracardiac puncture
96 after isoflurane anesthesia (IsoFlo, Veterinarian Esteve, Bologna, Italy). After blood collection,
97 rats were perfused using an isotonic solution of NaCl 0.9% to remove the remaining blood-
98 irrigating tissues, and then the heart and aorta were excised from the rats. All samples were
99 stored at –80 °C until analysis.

100 *Preparation of the SEC phenolic extract*

101 SEC extract (from the olive cake) was prepared as previously reported^{3,4,14}, with some
102 modifications. The phenolic composition of the SEC extract used can be found in Catalán et al.
103^{4,15}. Briefly, the phenolic composition of the SEC extract is mainly composed by dialdehydic
104 form of elenolic acid linked to hydroxytyrosol (3, 4-DHPEA-EDA; 40995.97 (1085.46) mg/kg
105 SEC extract) followed by HT (4176.82 (185.40) mg/kg SEC extract), isomer of oleuropein
106 aglycone (3,4- DHPEA-EA16; 28.98 (274.01) mg/kg SEC extract), dialdehydic form of elenolic
107 acid linked to tyrosol (*p*-HPEA-EDA; 936.37 (60.66) mg/kg SEC extract), oleuropein (480.00
108 (70.33) mg/kg SEC extract), and aldehydic form of elenolic acid linked to tyrosol (*p*-HPEA-EA;
109 378.82 (21.63) mg/kg SEC extract)⁴. To calculate the administered dose of 5 mg/kg weight of
110 SECs, we used 3, 4-DHPEA-EDA, which is considered to be the main SEC derivate producing
111 HT.

112 *Biochemical parameters*

113 Total cholesterol (TC), triglycerides (TGs), high-density lipoprotein cholesterol (HDLc), non-
114 HDLc, and glucose were measured in the rat plasma through standardized methods using a
115 Cobas Mira Plus autoanalyzer (Roche Diagnostics, Spain). Insulin was measured using a
116 Mercodia Rat Insulin Enzyme-linked ImmunoSorbent Assay (ELISA; reference 10-1250-10)
117 from AD Bioinstruments S.L. (Barcelona, Spain). TC, TGs, HDLc, non-HDLc, and Glucose are
118 expressed as mg/dL, and insulin is expressed as µg/L.

119 *Protein–protein interactions (PPIs)*

120 To examine the protein partners of FKBP1A and GJA1 (in the tissue of rat hearts or aortas,
121 respectively), a coimmunoprecipitation (Co-IP) experiment was completed in nondenaturing
122 conditions to preserve and thereafter analyze the potential PPIs.

123 *Protein isolation from aorta and heart tissues*

124 Heart and aorta tissues were carefully harvested, cleaned of connective tissue (in the case of the
125 aorta), snap-frozen, and stored at -80 °C until tissue lysis.

126 Heart tissues were homogenized with a micropestle in protein extraction lysis buffer (1 mg heart
127 tissue/30 μ L of protein extraction lysis buffer) provided by Pierce Crosslink
128 Immunoprecipitation kit 26147 plus a protease (cOmplete Mini 11836153001, Roche
129 Diagnostics GmbH, Germany) and phosphatase (cOmplete ULTRA Tablets, Mini, EDTA-free,
130 EASYpack 05892791001, Roche Diagnostics GmbH, Germany) inhibitor cocktail (1 tablet of
131 protease + 1 tablet of phosphatase inhibitor cocktail per 10 mL of lysis buffer). The homogenate
132 was then incubated at 4 °C with rotatory agitation for 2 h. Then the lysate was centrifuged at
133 13,000 x g for 10 min at 4 °C. The supernatant was recovered, and the total protein
134 concentration was measured using a Bradford assay. Samples were kept at -80 °C until the Co-
135 IP procedure.

136 Aortic tissues were ground into a powder using a ceramic mortar and pestle filled with liquid
137 nitrogen (-196 °C). The powder was transferred to a microcentrifuge tube, and then 400 μ L of
138 protein extraction lysis buffer (the same buffer used for the heart tissue homogenization) was
139 added. The homogenate was then incubated at 4 °C with rotatory agitation for 2 h. Samples were
140 homogenized and centrifuged at 21,000 x g for 30 min at 4 °C to pelletize the cell debris. The
141 supernatant was recovered, and the total protein concentration was measured using a Bradford
142 assay. Finally, samples were kept at -80 °C until the Co-IP procedure.

143 *Co-immunoprecipitation (Co-IP) assay*

144 Here, 10 μ g of commercial antibodies were covalently immobilized by crosslinking them with
145 protein A/G beads (following the antigen immunoprecipitation procedure of the Crosslink and
146 Immunoprecipitation Kit) (Pierce-Thermo Fisher Scientific). The antibody used for GJA1 in the
147 aortas was connexin 43 (F-7)/sc-271837 (Santa Cruz Biotechnology, USA), and the antibody
148 used for FKBP1A in heart tissue was FKBP12 (H-5)/sc-133067 (Santa Cruz Biotechnology,
149 USA). The antibodies were saturated with antigen to determine the levels of statistical
150 difference between partner proteins instead of simply the different expression levels of the
151 target bait proteins.

152 For each immunoprecipitation assay, a preclearing assay (a fraction of the lysate that interacted
153 with the A/G beads in the absence of antibodies) was performed before incubation (with the
154 antigen) of the antibody linked to the protein A/G beads to eliminate nonspecific binding
155 proteins. In addition, the negative control was also analyzed to indicate the nonspecific binding
156 proteins.

157 *Buffer exchange and protein digestion*

158 To perform a buffer exchange after the Co-IP procedure, 100 μ L of ammonium bicarbonate 50
159 mM Urea 2 M was added to the Co-IP eluates of the heart or aorta, loaded onto 10-kDa
160 Amicon® Ultra-0.5 devices, and centrifuged for 10 min at 21,000 $\times g$. This step was repeated
161 three times until the final sample volume was about 40 μ L. Then, the samples were reduced
162 with 4 mM dithiothreitol for 1 h at 37 °C, alkylated with 8 mM iodoacetamide for 30 min at 25
163 °C (in the dark), and digested overnight at 37 °C with trypsin (enzyme protein ratio of 1:100).

164 After digestion, samples were desalted on an Oasis hydrophilic–lipophilic balanced solid-phase
165 extraction column (Waters, Bedford, MA) using 75% acetonitrile (ACN), 25% water, and 0.1%
166 formic acid (FA) for elution. The eluted peptides were dried in a Speed-Vac and resuspended in
167 50 μ L of 0.1% FA before an analysis using a nanoLC-(Orbitrap) MS/MS.

168 *NanoLC-(Orbitrap) MS/MS analysis*

169 Here, 18 μ L of each sample was loaded on a trap nanocolumn (0.01 \times 2 cm, 5 μ m, Thermo
170 Fisher Scientific, San José, CA, USA) and separated onto a C-18 reversed-phase nanocolumn
171 (0.0075 \times 12 cm, 3 μ m, Nikkyo Technos Co., Ltd., Japan). The chromatographic separation was
172 performed through a 90-min gradient with Milli-Q water (0.1% FA) and ACN (0.1% FA) as the
173 mobile phase (at 300 nL/min). Mass spectrometry analyses were performed on an LTQ-Orbitrap
174 Velos Pro (Thermo Fisher Scientific, Madrid, Spain) through an enhanced Fourier-transform
175 (FT) resolution spectrum ($R = 30,000$ full width at half maximum; FWHM). This was followed
176 by ion-trap tandem mass spectrometry data-dependent scanning of the 10 most intense parent

177 ions, with a charge state rejection of 1 and a dynamic exclusion of 0.5 min at 35% normalized
178 collision energy using N₂ as a collision gas.

179 *Phosphoproteomic profiling*

180 *Protein extraction and quantification*

181 All of the aortic tissue was used for PPI analyses, and phosphoproteomic profiling was
182 conducted only in heart tissue. Heart tissue was weighed (80 mg approximately) prior to cell
183 lysis and protein extraction (following the radioimmunoprecipitation assay buffer protocol)
184 (ThermoFisher Scientific, Barcelona, Spain). Briefly, heart tissue was frozen with liquid
185 nitrogen and mixed with 1 mL of radioimmunoprecipitation assay buffer and completely
186 homogenized with a BlueBender with frozen/drawn cycles. It was then agitated for 1 h at 4 °C
187 and centrifuged at 21,000 x g for 5 min. After centrifugation, samples were sonicated with a 30-
188 s pulse at 50% amplitude. The samples were then centrifuged at 21,000 x g for 15 min, and
189 supernatants were collected for protein precipitation with the addition of 10% trichloroacetic
190 acid/acetone. The protein pellets were resuspended in 6 M urea/50 mM ammonium bicarbonate
191 and quantified using Bradford's method.

192 *Protein digestion*

193 Total proteins (500 µg) were reduced with 4 mM 1,4-dithiothreitol for 1 h at 37 °C and
194 alkylated with 8 mM iodoacetamide for 30 min at 25 °C in the dark. Afterward, samples were
195 digested overnight (pH 8.0, 37 °C) with sequencing-grade trypsin (Promega Biotech Ibérica SL,
196 Alcobendas, Madrid) at an enzyme/protein ratio of 1:50. Digestion was quenched through
197 acidification with 1% (v/v) FA, and peptides were desalted on an Oasis hydrophilic–lipophilic
198 balanced solid-phase extraction column (Waters, Bedford, MA) prior to phosphopeptide
199 enrichment.

200 *Phosphopeptide Enrichment and Mass spectrometry analyses*

201 Peptide mixtures were enriched with TiO₂ particles according to the High-Select TiO₂
202 Phosphopeptide Enrichment Kit protocol (ThermoFisher Scientific, Barcelona, Spain). Briefly,
203 peptides were suspended with Binding/Equilibration Buffer and were added to a TiO₂ Spin Tip
204 column, which had been previously conditioned. After phosphopeptide binding, the column was
205 washed, and the phosphopeptides were eluted with Elution Buffer. Samples were dried in a
206 speed vacuum and resuspended with 25 µL of water + 0.1% FA.

207 Mass spectrometry analyses were performed on an EasyII nanoLC coupled to an LTQ-Orbitrap
208 Velos Pro (both from Thermo Fisher) using an enhanced FT resolution MS spectrum ($R =$
209 30,000 FHMW). This was followed by data-dependent FT-MS/MS acquisition ($R = 7500$
210 FHMW, 40% higher energy collision dissociation) from the 10 most intense parent ions, with a
211 charge state rejection of 1 and a dynamic exclusion of 0.5 min. Chromatographic separation was
212 performed in reversed-phase mode on a C-18 reversed-phase nanocolumn (75-µm I.D.; 15-cm
213 length; 3-µm particle diameter, Nikkyo Technos Co., Ltd., Japan) with a 180-min gradient using
214 Milli-Q water (0.1% FA) and ACN (0.1% FA) as a mobile phase at a flow rate of 300 nL/min.

215 *Protein identification/quantification*

216 For PPIs and phosphoproteomics analyses, the raw data files were analyzed with Proteome
217 Discoverer software v.1.4.0.288 (Thermo Fisher Scientific, Madrid, Spain). For protein
218 identification, all MS and MS/MS spectra were analyzed using the Mascot search engine
219 (version 2.5), which was set up to search for *Rattus norvegicus* in the Swiss Prot database (8003
220 sequences) and the National Center for Biotechnology Information (NCBI) database (common
221 contaminants were used to remove possible false-positive findings). Two missed cleavages were
222 allowed, assuming trypsin digestion and a mass error of 0.8 Da for IT-MS/MS, 20 mmu for FT-
223 MS/MS, and 10.0 ppm for parent ions (FT-MS). The oxidation of methionine and acetylation of
224 the N-termini were set as dynamic modifications, and the carbamidomethylation of cysteine was
225 set as a static modification. For the phosphoproteomic experiments, the phosphorylation of
226 serine, threonine, and tyrosine was also set as a dynamic modification. The false discovery rate
227 and protein probabilities were calculated by Perclorator. For the PPI experiments, protein

228 quantification was based on a label-free approach, using the average area of the three most
229 intense unique peptides for each protein normalized by the sum of all proteins after the proteins
230 were filtered, selecting only those proteins that were identified in at least 50% of at least 1 out
231 of 2 conditions. In addition, any highly abundant blood proteins identified in the PPI
232 experiments were eliminated, since these were the result of blood remaining after tissue
233 perfusion. The proteins identified in the PPI negative controls (Co-IP purification of tissue
234 extracts without antibodies) were also eliminated. For phosphoproteomics analyses,
235 quantification was performed using the label-free approach, but at the peptide level (using the
236 chromatographic peak area of the identified peptides).

237 The MS proteomics data were deposited in the ProteomeXchange Consortium via the PRIDE ¹⁶
238 partner repository, with the dataset identifier PXD017841.

239 No western blot confirmation for proteins was conducted in this study due to the findings of
240 Aebersold R. et al., who confirmed that results obtained through MS-based proteomics (also
241 recognized by the journal *Nature Methods* as the “method of the year” for 2012 ¹⁷) are vastly
242 superior to those obtained through western blot for several reasons: we thus felt it was not
243 necessary ¹⁸. Moreover, analyses of individual biological replicates (instead of pooled samples),
244 as was the case in our study, lead to higher statistical confidence about differentially expressed
245 proteins and make the use of additional methods to validate findings unnecessary.

246 *Statistical Analyses*

247 To discover the significant protein changes between the different conditions, Mass Profiler
248 Professional software v.14.5 (Agilent Technologies, Barcelona, Spain) was used. The data were
249 Log₂-transformed and mean-centered for multivariate analyses (Principal Component Analysis
250 and Hierarchical Clustering Analysis) and univariate statistical analyses (Student’s *t*-test). Here,
251 $p < 0.05$ was considered to be statistically significant.

252 Before statistical analyses of the PPI results, the protein list was further filtered to avoid false-
253 positive findings by selecting only those proteins that were quantified in 100% of at least 1 out

254 of the 2 conditions. For the phosphoproteomics profiling results, the peptide list was further
255 filtered to avoid false-positive findings by selecting only those proteins that were quantified in
256 at least 75% of at least 1 out of the 2 conditions (568 peptides). Missing values were replaced
257 with a small value estimated as the limit of detection (10^4 area) to perform the statistical
258 analyses ($p < 0.05$).

259 Fold Change (FC) was calculated by dividing the average raw values for SEC group by CTRL
260 group, except for $FC < 1$, that was recalculated as $1/FC$ and indicated as “-“. This representation
261 was used to simplify FC magnitude interpretation (positive for absolute up-regulation and
262 negative for absolute down-regulation).

263 *Clustering and pathway analyses*

264 The initial functional evaluation was performed using the UniProt (www.uniprot.org) database,
265 with a focus on protein function and relevant biological processes.

266 Ingenuity Pathway Analysis (IPA software; Ingenuity System Inc., Redwood, CA, USA;
267 www.ingenuity.com) was employed to examine the functional correlations within the SEC and
268 control groups. Datasets containing protein identifiers (UniProt-KB) and corresponding
269 expression values (FC) of the two comparative groups (SEC vs control) were uploaded. Each
270 protein identifier was mapped to its corresponding protein object in the Ingenuity Pathways
271 Knowledge Base. All mapped proteins were differentially expressed at $p < 0.05$ and overlapped
272 onto global molecular networks developed from information contained in the knowledge base.
273 The networks were then algorithmically generated based on their connectivity and “named” in
274 terms of the most prevalent functional group(s) present within them. The networks were ranked
275 by a score that defined the probability of a collection of nodes being equal to or greater than that
276 number achieved by chance alone. Canonical pathways, Diseases, BioFunctions, Ingenuity Tox
277 List, and Molecule Activity Predictor tools were overlapped on the networks.

278 **RESULTS**

279 *Serum lipid and glucose biomarkers in rats*

280 After the SEC treatment, there were no significant differences found between female Wistar rats
281 fed 5 mg of SECs/kg rat weight/day compared to the control group fed only with the standard
282 diet in terms of the biochemical parameters of TC, TGs, HDLc, non-HDLc, glucose, or insulin
283 (**Table 1**).

284 *PPIs of FKBP1A in rat heart tissues and GJA1 in rat aortic tissues*

285 A list of the proteins identified in the study of FKBP1A in rat heart tissue (213 in total) and the
286 proteins identified in GJA1 in rat aortic tissue (358 in total) is included in **Supplementary**
287 **Table 1** and **Supplementary Table 2**, respectively. The Tables contain information regarding
288 protein identification (ID; UniProt accession number), protein name, coverage, Mascot Score,
289 Protein groups, Unique peptides identified, total peptides identified, the number of amino acids
290 in the protein sequence, protein molecular weight, and calculated isoelectric point. In addition,
291 quantification results are included, reported as the surface area of each of the 213 identified
292 proteins in the rat heart tissue or the 358 identified proteins in the rat aortic tissue.

293 The samples from each type of tissue were very similar, but the samples coming from the SEC
294 and control groups were different from each other. The similarity of samples indicates that all
295 analyses were successfully performed and all of the data could be statistically analyzed.

296 Thirteen significant proteins physically interacted with FKBP1A, but this differed depending on
297 the group (the SEC or control group) ($p < 0.05$). We observed a significant increase in TNNT3,
298 ACAT1, HSPA5, HPRT1, ACYP2, HIST1H1D, ATP8, SUCLG1, YWHAZ, and PHB2
299 proteins and a decrease in IGHG1, HSPE1, and CRIP2 proteins in the SEC group compared to
300 the control group. The significant proteins, their p -values, and their FCs (for both the SEC and
301 control groups) are detailed in **Table 2**.

302 Twenty-seven significant proteins interacted with GJA1, but this differed depending on the
303 group (the SEC or control group) ($p < 0.05$). We observed a significant increase in NDUFV2,
304 IGKC, Ig lambda-2 chain C region, IGH-1A, SELENBP1, and Ig heavy chain V region IR2

305 proteins and a decrease in ERP29, DLD, CAPNS1, ARF3, TUBA1A, TUBA1B, VCP,
306 YWHAQ, HSD17B4, YWHAB, ANXA2, DES, CNN1, YWHAZ, ACTN4, HSPB1, RPS18,
307 RAN, HBA1, DSTN, and CFL1 proteins in the SEC group compared to the control group. The
308 significant proteins, their *p*-values, and their FCs (for both the SEC and control groups) are
309 detailed in **Table 3**.

310 Using IPA software, we identified the subcellular localization of the significant proteins that
311 physically interacted with FKBP1A and GJA1, which was different depending on the group (the
312 SEC or control group). We found that in heart tissue, 61.5% of these proteins (eight proteins
313 that interacted with FKBP1A) were located in the cell cytoplasm, 7.7% (*n* = 1) were in the
314 nucleus, 7.7% (*n* = 1) were in the plasma membrane, and the remaining 23.1% (*n* = 3) did not
315 have any subcellular localization information available in this database (**Table 2**). In aortic
316 tissue, 70.4% of these proteins (19 proteins that interacted with GJA1) were located in the cell
317 cytoplasm, 7.4% (*n* = 2) were in the nucleus, 3.7% (*n* = 1) were in the plasma membrane, and
318 there was no available information in the IPA software for the remaining 18.5% (*n* = 5) (**Table**
319 **3**).

320 *Cardiovascular Disease Network of PPIs in rat heart and aortic tissues*

321 When the complete dataset of proteins that were differentially expressed in the heart was
322 analyzed, the predominant network found by IPA was “Cardiovascular Disease” (score = 18).
323 Eight of the thirteen proteins that interacted with FKBP1A were part of this network (HSPE1,
324 CRIP2, PHB2, ACAT1, SUCLG1, YWHAZ, HSPA5, and TNNT3). The predominant networks
325 of proteins that were differentially expressed in the aorta (found by IPA) were “Cardiovascular
326 Disease”, “Neurological Disease”, and “Cancer” (score = 24). Thirteen of the twenty-seven
327 proteins that interacted with GJA1 were part of this network (NDUFV2, ANXA2, DLD,
328 TUBA1A, YWHAB, CALPAIN, CFL1, RAN, HSPB1, YWHAZ, DSTN/DSTNL1, VCP, and
329 HSD17B4).

330 A graphical representation of the PPI network is shown in **Figure 1** (heart tissue) and **Figure 2**
331 (aortic tissue). The modulated proteins (located in the cell compartments) are highlighted (red
332 means upregulated and green means downregulated), which indicates whether the proteins in
333 the SEC group were up- or downregulated compared to the control group. Violet lines indicate
334 the physical PPIs associated with FKBP1A in the heart or GJA1 in the aorta, and the figure
335 shows how different proteins interact with each and how they are involved within the same
336 network.

337 Molecules and lines highlighted in orange or blue show predicted activation or inhibition,
338 respectively, which were obtained from IPA based on the expected effects between
339 transcriptional regulators and their target genes (information stored in the Ingenuity®
340 Knowledge Base).

341 As is shown in **Figure 1**, GATA4 and P38MAPK seemed to be the main activators of TNNI3 or
342 HSPA5, respectively, as observed in the heart tissue. Furthermore, **Figure 2**, which shows
343 aortic rat tissue, shows that the predicted activation of CTNNA1 seemed to be regulated by
344 decreased calpain proteins; further, the predicted activation of TSC2 led to the inhibition of
345 CRYAB, HSPB1, and ANXA2. On the other hand, IPA showed that in our protein dataset,
346 CRYAB, Tpm1, MAPK14, and NOS2 were inhibited in aortic rat tissue.

347 *Upstream regulators of PPIs in rat heart and aortic tissues were network interactions*

348 The IPA upstream regulators identified a cascade of upstream transcriptional regulators, which
349 could explain the gene expression changes observed in the protein dataset. In heart tissue, the
350 top five upstream regulators in the protein dataset were MYC, GATA4, TNNI1, EPHX2, and
351 PDIA6. However, in aortic tissue, the top five upstream regulators in the protein dataset were
352 S100A1, KDR, TSC2, calpain, and NOS2. These regulators helped to illuminate the biological
353 activities occurring in the tissues and cells.

354 *Major relevant diseases and biological functions of PPIs in rat heart and aortic tissue*

355 **Table 4** lists the relevant diseases and biological functions of proteins in rat heart and aortic
356 tissue, including those proteins that physically interact with FKBP1A or GJA1 and are involved
357 mainly in the “Cardiovascular Disease” network. The main diseases and functions identified by
358 the PPI analysis were cardiovascular disease, cardiovascular system development and function,
359 metabolic disease, lipid metabolism, inflammatory disease, inflammatory response, cancer, free-
360 radical scavenging, neurological disease, immunological disease, gastrointestinal disease, and
361 hepatic system disease.

362 *Heart phosphoproteomic profile of rats*

363 A total of 635 phosphopeptides and 415 phosphorylated proteins were identified in the rat heart
364 tissue. After filtering the peptides by frequency (75% in at least one group), 568 phosphorylated
365 peptides were (confidently) found in the samples and were used for statistical purposes
366 (**Supplementary Table 3**). First, regarding an overall performance analysis, principal
367 component analysis and clustering showed that the overall samples were very similar, and no
368 outliers were detected. However, the samples coming from the SEC and control groups were
369 different from each other (data not shown). After a univariate statistical analysis (Student’s *t*-
370 test), 29 peptides were found to be significant ($p < 0.05$), differing between groups (**Table 5**).
371 The changes in expression levels for those proteins containing significant phosphopeptides
372 (assessed in previous work ⁴) indicate the proteins identified that contained phosphopeptides.
373 No significant changes were found between the SEC and control groups, indicating that changes
374 in the functionality/activity of these proteins were not due to protein over- or subexpression. In
375 the rat hearts, we observed a significant increase in the phosphorylation of SRRM1, LRRC47,
376 GAB2, MAP4, JPH2, RAPH1, NUFIP2, SVIL, PROB1, TNIK, PGAM1, NACA, and
377 HIST1H4B. In addition, there was a decrease in phosphorylation of DMTN, TCEA1, SZRD1,
378 MAP1A, HRC, MYLK3, EEF1D, OBSCN, PTGES3L, PGRMC1, CTNNA1, AKT1S1,
379 PPP1R2, CARHSP1, GJA1, and LOC683897 in the SEC group compared to the control group.
380 Significant phosphorylated peptide sequences, their corresponding proteins, their biological
381 processes, their molecular functions, their *p*-values, the phosphorylated FCs, and the serine

382 phosphorylation sites for the SEC group versus the control group are detailed in **Table 5**. Using
383 IPA software, the subcellular localization of the phosphorylated proteins was identified. We
384 found that 55.17% (16 phosphorylated proteins) were located in the cell cytoplasm, and 20.69%
385 (6 phosphorylated proteins) were in the plasma membrane. Further, 10.34% ($n = 3$) were
386 mapped as nuclear phosphorylated proteins, and there was no subcellular localization
387 information available in the database for the remaining 13.79% (four phosphorylated proteins)
388 (**Supplementary Figure 1**).

389 The major canonical pathways of the phosphorylated proteins in the SEC group—which were
390 modified by SEC treatment—were compared to the control. The main phosphorylated proteins
391 involved in their regulation (obtained by IPA analysis) were Endometrial Cancer signaling
392 (CTNNA1, GAB2), Rapoport-Luebbing Glycolytic Shunt (PGAM1), Endocannabinoid
393 Developing Neuron pathway (AKT1S1, GAB2), 14-3-3-mediated signaling (AKT1S1, GAB2),
394 Ovarian Cancer signaling (GAB2, GJA1), mTOR signaling (AKT1S1, GAB2), and Gap Junction
395 signaling (GAB2, GJA1).

396 *The integrated network between heart PPIs and phosphoproteome analyses*

397 We then proceeded to establish a relationship between the PPIs associated with FKBP1A and
398 the main phosphorylated proteins: this was to integrate everything into a unique Network. The
399 top Cardiovascular Disease Network found by IPA was “Cardiovascular System Development
400 and Function” (Score = 23).

401 A graphical representation of the integrated network of heart FKBP1A PPIs + the heart
402 phosphoproteome is shown in **Figure 3**, in which modulated proteins (located in the cell
403 compartments) are highlighted in red or green (indicating whether the phosphorylated proteins
404 in the SEC group were up- or downregulated compared to the control group, respectively).
405 Moreover, violet lines indicate the physical PPIs with FKBP1A in rat hearts, showing how the
406 proteins were connected and how they were involved in the same network.

407 **DISCUSSION**

408 The protective role against cardiovascular disease that SECs, mainly composed by 3, 4-
409 DHPEA-EDA, HT, 3,4- DHPEA-EA, p-HPEA-EDA, oleuropein, and p-HPEA-EA, exert has
410 been widely reported through in vitro and in vivo studies and clinical trials: this research has
411 focused mainly on SECs' antioxidant capacity, their ability to modulate cellular antioxidant
412 defense mechanisms, and their anti-inflammatory activities. Secoiridoids have been
413 demonstrated to modulate different targets such as iNOS, NO, TNF α , MMP-2, MMP-9,
414 VCAM-1, and ICAM-1 and to modulate signaling pathways by altering, e.g., MAPK, NF κ B,
415 and Nrf2/HO-1^{15,19}. Information is limited on the effects of SECs on a proteomic level;
416 however, one previous study of ours was based on descriptive proteomics and was the first to
417 confirm changes at the proteomic level in cardiovascular tissues (aorta and heart) related to the
418 proliferation and migration of endothelial cells and heart failure in female Wistar rats⁴. Other
419 changes have also been reported after SEC dietary supplementation in rodent models in adipose
420 and liver tissue proteomes: these changes were related to lipid metabolism and an oxidative
421 stress response²⁰. The present study is the first to go a step further and observe SECs' effects on
422 PPIs associated with GJA1 in female rat aortas and with FKBP1A in female rat heart tissue.
423 Further, we explored the phosphoproteomic profile of key proteins in female rat heart tissue,
424 which may explain or implicate the up-/downregulation of proteins in the different major
425 canonical pathways: this may be related to cardiovascular disease.

426 *Heart*

427 In rat heart tissue affected by SEC consumption (compared to the control diet), eight of the
428 differentially expressed proteins had direct PPIs with FKBP1A (related to the cardiovascular
429 disease network). Two out of the eight proteins, HSPE1 and CRIP2, were downregulated in the
430 heart network. Meanwhile, the other six—PHB2, ACAT1, SUCLG1, HSPA5, TNNI3, and
431 YWHAZ—were upregulated in the heart network.

432 The mitochondrial 10-kDa heat shock protein (**HSPE1**) is a co-chaperonin implicated in
433 mitochondrial protein importation and macromolecular assembly. Together with Hsp60, it

434 facilitates the correct folding of imported proteins. The role of this protein in heart tissue is
435 unknown, but some literature on cancer has shown that the repression of proteins related to cell
436 survival (such as HSPE1, HSPB1, and HSPA5) can suppress tumorigenic ability and the
437 motility/invasiveness of breast cancer cells through the overexpression of profilin-1 ²¹.

438 Cysteine-rich protein 2 (**CRIP2**) is highly expressed during cardiovascular development and
439 can act to bridge the serum response factor and GATA proteins and to stimulate smooth muscle
440 target genes ²¹. The expression of CRIP2 is upregulated in myocardial infarction, so a decrease
441 in this protein due to SECs could be associated with a potentially relevant gene in the pathology
442 of myocardial infarction ²².

443 Mitochondrial acetyl-CoA acetyltransferase (**ACAT1**) converts cellular cholesterol into
444 cholesteryl ester in response to cholesterol abundance. In atherosclerotic lesions, where
445 macrophages ingest excess cholesterol, the ability to esterify newly acquired cholesterol seems
446 to be important for cell survival. The inhibition of ACAT1 may bring about undesired
447 consequences, with the destabilization of cellular membrane functions due to cholesterol
448 accumulation leading to macrophage cell death ²³. We found in this study that ACAT1
449 interacted with FKBP1A in heart tissue, and in a study by Denuc and coworkers, it was found
450 that ACAT1 interacted with GJA1 in the same tissue ²⁴, which suggests that FKBP1A and GJA1
451 could be integrated in a similar pathway (this was found in this study as well but in different
452 tissue). SECs thus induce an increase in ACAT1 protein concentrations.

453 The upregulation of mitochondrial Succinate-CoA ligase subunit alpha (**SUCLG1**) protects
454 cardiomyocytes from oxidative injury ²⁵. Here, SECs had a positive effect, inducing the
455 upregulation of the SUCLG1 protein.

456 Endoplasmic reticulum chaperone BiP (**HSPA5**) plays a key role in protein folding in newly
457 formed proteins and in quality control in the endoplasmic reticulum lumen. Reduced levels of
458 HSPA5 (or calcium overload in the endoplasmic reticulum (ER)) cause proteins to unfold and

459 produce an ER stress response ²⁶. As observed in our study, SECs may have beneficial effects
460 that help increase HSPA5 levels.

461 Cardiac Troponin I (**TNNI3**) helps coordinate the contraction of the heart. It has been
462 demonstrated that TNNI3 mutation causes variable phenotypic expressions, such as restrictive
463 cardiomyopathy (RCMP) or hypertrophic cardiomyopathy (HCMP) ²⁷. Therefore, SECs can
464 maintain elevated TNNI3 levels to prevent RCMP or HCMP.

465 It was recently demonstrated that 14-3-3 protein zeta/delta (**YWHAZ**), an adapter protein
466 implicated in the regulation of a large spectrum of both general and specialized signaling
467 pathways, is involved in cardiovascular disease ²⁸, but further studies are needed. Previous
468 studies in other tissues (not the heart or aorta) have led to differing results regarding its up- or
469 downregulation. The knockdown of YWHAZ promotes both in vitro and in vivo tumorigenesis
470 in bladder cancer and may be a novel biomarker for bladder cancer, an idea that deserves further
471 study ²⁹. Another study conducted with rutin (a flavonoid-type phenolic compound) showed that
472 rutin treatment protects against UVA-induced increases in the total expression of proteins
473 involved in the inflammatory response, such as YWHAZ ³⁰ (this is similar to our results, where
474 SECs caused an increase in YWHAZ in heart tissue). Other studies of breast cancer have shown
475 an increase in YWHAZ ³¹ or an overexpression of YWHAZ in adenocarcinoma of the
476 esophagogastric junction, where patients with YWHAZ-overexpressed tumors had worse
477 overall survival rates than did those with tumors with a lower expression. Given our results, it
478 may be useful as a prognosticator and potential therapeutic target and indicator ³² (in aortic
479 tissues, SECs decreased YWHAZ). However, other studies have shown no significant
480 differences between tumoral and normal gastric tissue in terms of YWHAZ gene expression,
481 which is similar to what we observed in our study ³³. For this reason, and due to the discrepancy
482 observed in the up- or downregulation of YWHAZ in different tissues or pathologies, further
483 studies in different tissues should be performed.

484 Prohibitin-2 (**PHB2**) is a novel antiproliferative protein that plays a role in cellular senescence,
485 apoptosis, and the maintenance of mitochondrial function in mammals. The name Prohibitin
486 refers to the negative effects of these proteins on cell proliferation. It has been observed in
487 previous studies that PHB2 is aberrantly expressed in cancers such as neuroblastoma, breast
488 cancer, liver cancer, ovarian cancer, and thyroid cancer³⁴, but its effects in cardiac tissue have
489 not been studied. For this reason, it is important to conduct new studies on its effects on the
490 heart and how SECs could have an effect by increasing its expression.

491 *Aorta*

492 In the aortic tissue of rats fed SECs (compared to the control diet), 13 of the total differentially
493 expressed proteins had a direct PPI with GJA1, as they related to the cardiovascular disease
494 network. One out of the thirteen proteins, NDUFV2, was upregulated in the aortic network.
495 Meanwhile, the other 12 proteins, ANXA2, DLD, TUBA1A, VCP, YWHAZ, YWHAB,
496 HSD17B4, Dstn/Dstnl1, HSPB1, RAN, CFL1, and Calpain, were downregulated in the aortic
497 network.

498 Mitochondrial NADH dehydrogenase (ubiquinone) flavoprotein 2 (**NDUFV2**) was the only
499 protein that was upregulated in the aortic network of rats given an SEC diet. NDUFV2 is a core
500 subunit of the mitochondrial membrane respiratory chain NADH dehydrogenase (Complex I)
501 and is responsible for transferring electrons from NADH to the respiratory chain. PTMs of the
502 NDUFV2 subunit of complex I in the heart (specifically, the phosphorylation of Tyr118
503 residue) have been proposed to exert positive effects by inhibiting complex I activity and
504 ameliorating mitochondrial oxidative stress³⁵.

505 Different cell types, including smooth muscle cells and endothelial cells, express Annexin A2
506 (**ANXA2**). It has been suggested that an alteration in endothelial cells that leads to a reduction
507 in ANXA2 expression may lead to a predisposition to cardiovascular disease³⁶. Moreover,
508 lower ANXA2 levels are related to an increase in the plasma levels of PCSK9, and thus increase

509 LDL-c levels and the risk of coronary heart disease ³⁷. The role played by a decrease in ANXA2
510 in aortic tissue after SEC treatment should be studied in future research.

511 We observed a downregulation of mitochondrial dihydrolipoyl dehydrogenase (**DLD**) due to
512 SEC treatment: this protein is known to be associated with neurological diseases such as
513 Alzheimer's disease ³⁸. The major network proteins derived from the aortic tissue analysis were
514 related both to neurological diseases and cardiovascular disease. However, the relation of DLD
515 to cardiovascular disease has not been described in the literature, and future studies will need to
516 interpret our results.

517 Tubulin alpha-1A chain (**TUBA1A**) is a structural constituent of the cytoskeleton and
518 participates in structural molecule activity. TUBA1A has been identified in adipose tissue as a
519 novel candidate gene for obesity, which implies a role in fat cell functioning ³⁹. Therefore, SECs
520 could have a role in fat cell functioning through the modification of TUBA1A expression.
521 However, this is a speculative hypothesis, since no evidence has been published about the role
522 of TUBA1A in aortic tissue.

523 Valosin-containing protein (**VCP**), an ATPase associated with various cellular activities, is
524 ubiquitously expressed in cells and has been implicated in multisystem degenerative disorders.
525 VCP has been previously identified in heart tissue, and its downregulated expression has been
526 linked to hypertensive cardiomyopathy ⁴⁰. Moreover, the overexpression of VCP in isolated
527 cardiac myocytes promotes cardiac survival through the activation of NF-κB and a dose-
528 dependent increase in inducible nitric oxide synthase (iNOS) expression ⁴¹. In our study, VCP
529 was downregulated after SEC treatment, which should mean it does not have cardioprotective
530 effects; however, more studies are necessary.

531 Unlike the **YWHAZ** overexpression observed in the heart tissue after SEC treatment, this
532 protein was downregulated in aortic tissue. As discussed above, due to discrepancies in terms of
533 its up- or downregulation (in different tissues), further studies should be performed.

534 In addition, 14-3-3 protein beta/alpha (**YWHAB**) is an adapter protein implicated in the
535 regulation of a large spectrum of both general and specialized signaling pathways. YWHAB has
536 recently been proposed as a diagnostic biomarker and a therapeutic target for vascular
537 complications, as its inhibition may alleviate intimal hyperplasia following carotid artery injury,
538 therefore suppressing endothelial cell proliferation and migration ⁴². SECs could thus have
539 vascular beneficial effects, helping to decrease YWHAB levels.

540 Peroxisomal multifunctional enzyme type 2 (**HSD17B4**) is an enzyme acting in the peroxisomal
541 beta-oxidation pathway for fatty acids. HSD17B4 has been observed to be overexpressed in
542 prostate cancer cells. Moreover, the selective inhibition of HSD17B4 has been demonstrated to
543 inhibit cancer cell proliferation, suggesting that HSD17B4 is a novel biomarker and drug target
544 for cancer therapeutics ⁴³. Here, the downregulation of HSD17B4 after SEC treatment shows
545 that phenolic compounds have a possible antineoplastic effect.

546 Heat shock protein beta-1 (**HSPB1**) is a small chaperone that plays a role in maintaining
547 denatured proteins in a folding-competent state and in maintaining redox homeostasis. HSPB1
548 exhibits robust expression in the myocardium and blood vessels, and for this reason, its role in
549 the cardiovascular system is important. HSPB1 and other HSPs are significantly more expressed
550 in stressed hearts; however, the possible beneficial or deleterious effects of cardiomyocytes
551 (through increased levels of HSPB1) remain unclear ⁴⁴. Therefore, to correctly interpret the
552 meaning of the HSPB1 downregulation we observed after SEC treatment, more studies are
553 needed.

554 GTP-binding nuclear protein Ran (**RAN**), which is involved in nucleocytoplasmic transport,
555 plays a critical role in the import of cargo proteins into the nucleus. Here, it was downregulated
556 after SEC treatment. Vascular smooth muscle cell (VSMC) proliferation is a key component of
557 vascular pathologies, such as hypertension and atherosclerosis, and it can be modulated by a
558 mechanism that involves the stimulation of nuclear protein importation through interaction with

559 Ran. This cellular signaling, which also implicates Hsp60, may be important in growth-based
560 vascular pathologies ⁴⁵.

561 The destrin (**DSTN**) and cofilin-1 (**CFL1**) families are involved in the regulation of the actin
562 cytoskeleton and play crucial roles in development, tissue homeostasis, and disease ⁴⁶. We
563 observed a decrease in cofilin-1 (**CFL1**) in the tissue of rats given SEC treatment; further, it has
564 been previously proven that CFL1 actin-binding protein deletion could inhibit NF-κB activity
565 via cytoskeletal remodeling, modulating inflammation and blood pressure ⁴⁷.

566 Calpains are a group of nonlysosomal Ca²⁺-dependent cysteine proteases with numerous
567 substrates. Calpains are involved in different physiological and pathological processes, such as
568 cell proliferation, migration, invasion, apoptosis, and signal transduction ⁴⁸. Calpain inhibition
569 was recently linked to the suppression of macrophage migration to adipose tissue, attenuating
570 adipose tissue inflammation and fibrosis ⁴⁹. Here, the downregulation of Calpain small subunit-1
571 (**Capns1**) after SEC treatment indicates it could be a possible new therapeutic target to reduce
572 obesity-induced adipose tissue inflammation.

573 *Final remarks*

574 In studying PPIs and the phosphoproteome in the same sample at the same time, some common
575 and important protein PTMs could be determined, including information on the protein's state
576 of activity, localization, turnover, and interaction with other proteins ⁵⁰. However, there are
577 other PTMs that were not determined in this study but that could be important for determining
578 the state of activity, including acetylation, methylation, and glycosylation. Today, no proteomic
579 method exists that can determine all PTMs existing at the same time and in the same sample,
580 and this is something that should be rectified using high-throughput technologies in future
581 years.

582 On the one hand, increases in peptidyl-prolyl cis-trans isomerase (**FKBP1A**) in heart tissue (due
583 to SEC treatment) are key for the regulation of the intracellular signaling pathways involved in
584 ventricular trabeculation and compaction ⁵¹. On the other hand, decreases in the Gap junction

585 alpha-1 protein (**GJA**) in the aortic tissue (due to SEC treatment) could regulate the
586 proliferation of endothelial cells, as well as the initiation and development of atherosclerosis ¹⁰.
587 Moreover, the downregulation of GJA1 in aortic rat tissue (due to SEC treatment) was
588 confirmed through the phosphoproteome analysis conducted in the heart tissue, where we found
589 a significant downregulation in the phosphorylation of GJA1. In considering the ingenuity
590 analysis, we hypothesize that this reduction in the phosphorylation of GJA1 in the heart could
591 have been due to the predicted inhibition of the cascade of members of the catenin family, such
592 as CTNNB1 and CTNNA1 (found to be phosphorylated in our phosphoproteome analysis),
593 which happened through the inhibition of PKA, ERK1/2, and NOS2 (the same prediction we
594 observed in the reduction of the GJA1 protein in aortic tissue).

595 During the phosphoproteome analysis in the heart, we found a decrease in AKT1S1
596 phosphorylation and an increase in GAB2 phosphorylation. Both of these proteins are involved
597 in the activation of the canonical PI3K/mTOR signaling pathway and could play a protective
598 role in cardiomyocyte and cardiac functioning, as was shown in a recent study through low
599 concentrations of rutin treatment, another phenolic compound ⁵². Another important canonical
600 pathway that could be regulated by SECs is the Gap Junction signaling pathway, which is
601 regulated by an increase in GAB2 and a decrease in GJA1 phosphorylation. There are not many
602 relevant findings regarding GAB2 and its relation to Cardiovascular disease, but it is known that
603 GAB2 in the myocardium is essential for both the maintenance of myocardial functioning and
604 the stabilization of cardiac capillary and endocardial endothelia in the postnatal heart ⁵³.

605 Additionally, GJA1 is predicted to be the top key driver of an astrocyte-enriched subnetwork
606 associated with Alzheimer's disease (AD) ⁵⁴, and a reduction in this protein and the
607 phosphorylation of GJA1 through SEC treatment could be a promising pharmacological target
608 for AD.

609 The results of this study were obtained from a healthy rat model elucidating how SECs are
610 involved in cardiovascular disease prevention. A further step will be to confirm through a
611 cardiovascular disease rat model if SECs intake is also effective in cardiovascular disease

612 treatment. Another key point in the present study is gender. This study was conducted in healthy
613 female Wistar rats, so further studies in male Wistar rats are needed to corroborate the results.
614 Summarizing, there were PPIs associated with FKBP1A and GJA1, and the phosphoproteome
615 analysis conducted in this study through SEC treatment (mainly composed by 3, 4-DHPEA-
616 EDA) in healthy female rat tissues indicated promising proteins that could help identify new
617 drug targets that could mimic clinical benefits. This opens up the opportunity to test
618 physiologically relevant changes in the canonical PI3K/mTOR and Gap junction signaling
619 pathways (proposed to promote cardiovascular protection), which could explain the healthy
620 benefits of VOO.

621 **ABBREVIATIONS USED**

622 **ACN**, acetonitrile

623 **Co-IP**, co-immunoprecipitation

624 **Cx43**, connexin 43

625 **ELISA**, enzyme-linked immuno sorbent assay

626 **FA**, formic acid

627 **FC**, fold change

628 **FHMW**, full half-maximum width

629 **FKBP1A**, peptidyl-prolyl, cis-trans isomerase

630 **GJA1**, gap junction alpha-1 protein

631 **HDLc**, density lipoprotein cholesterol

632 **HT**, hydroxytyrosol

633 **IPA**, ingenuity pathway analysis

634 **nLC-MS/MS**, nano liquid chromatography coupled to tandem mass spectrometry

635 **PPI**, protein-protein interactions

636 **PTMs**, post-translational modifications

637 **SEC**, secoiridoids

638 **TC**, total cholesterol

639 **TG**, triglycerides

640 **VOO**, virgin olive oil

641 **ACKNOWLEDGMENT**

642 We thank the support of *Institut d'Investigació Sanitària Pere Virgili (IISPV)* and *Centre*
643 *Tecnològic de Nutrició i Salut (CTNS)* from *Fundació EURECAT*, Reus, Spain. NFOC-Salut
644 group is a consolidated research group of *Generalitat de Catalunya*, Spain (2014 SGR 873 and
645 2017 SGR 522). We also thank Maria Guirro and Elisabet Foguet from the Proteomics facility
646 of the Centre for Omic Sciences (COS) Joint Unit of the Universitat Rovira i Virgili-Eurecat,
647 for their contribution to mass spectrometry analysis.

648 **SUPPORTING INFORMATION DESCRIPTION**

649 **Supporting information Figure S1. Sub-cellular localization of the phosphorylated**
650 **proteins.** Each category and the relative percentage of the phosphorylated proteins present in
651 that category is shown as a pie chart.

652 **REFERENCES**

- 653 (1) Servili, M.; Sordini, B.; Esposito, S.; Urbani, S.; Veneziani, G.; Di Maio, I.; Selvaggini,
654 R.; Taticchi, A. Biological Activities of Phenolic Compounds of Extra Virgin Olive Oil.
655 *Antioxidants* **2014**, *3* (1), 1–23. <https://doi.org/10.3390/antiox3010001>.
- 656 (2) Celano, R.; Piccinelli, A. L.; Pugliese, A.; Carabetta, S.; Di Sanzo, R.; Rastrelli, L.;
657 Russo, M. Insights into the Analysis of Phenolic Secoiridoids in Extra Virgin Olive Oil.

- 658 *J. Agric. Food Chem.* **2018**, *66* (24), 6053–6063.
659 <https://doi.org/10.1021/acs.jafc.8b01751>.
- 660 (3) López de las Hazas, M. C.; Piñol, C.; Macià, A.; Romero, M. P.; Pedret, A.; Solà, R.;
661 Rubió, L.; Motilva, M. J. Differential Absorption and Metabolism of Hydroxytyrosol
662 and Its Precursors Oleuropein and Secoiridoids. *J. Funct. Foods* **2016**, *22*, 52–63.
663 <https://doi.org/10.1016/j.jff.2016.01.030>.
- 664 (4) Catalán, Ú.; Rubió, L.; López de Las Hazas, M. C.; Herrero, P.; Nadal, P.; Canela, N.;
665 Pedret, A.; Motilva, M. J.; Solà, R. Hydroxytyrosol and Its Complex Forms
666 (Secoiridoids) Modulate Aorta and Heart Proteome in Healthy Rats: Potential Cardio-
667 Protective Effects. *Mol. Nutr. Food Res.* **2016**, *60* (10), 2114–2129.
668 <https://doi.org/10.1002/mnfr.201600052>.
- 669 (5) Martín-Peláez, S.; Covas, M. I.; Fitó, M.; Kušar, A.; Pravst, I. Health Effects of Olive
670 Oil Polyphenols: Recent Advances and Possibilities for the Use of Health Claims.
671 *Molecular Nutrition and Food Research*. Mol Nutr Food Res May 2013, pp 760–771.
672 <https://doi.org/10.1002/mnfr.201200421>.
- 673 (6) de Roos, B.; McArdle, H. J. Proteomics as a Tool for the Modelling of Biological
674 Processes and Biomarker Development in Nutrition Research. *Br. J. Nutr.* **2008**, *99*
675 *Suppl 3*, S66-71.
- 676 (7) Morel, S. Multiple Roles of Connexins in Atherosclerosis- and Restenosis-Induced
677 Vascular Remodelling. *Journal of Vascular Research*. 2014, pp 149–161.
678 <https://doi.org/10.1159/000362122>.
- 679 (8) Chen, L.; Chen, Z.; Ge, M.; Tang, O.; Cheng, Y.; Zhou, H.; Shen, Y.; Qin, F. Monocytic
680 Cell Junction Proteins Serve Important Roles in Atherosclerosis via the Endoglin
681 Pathway. *Mol. Med. Rep.* **2017**, *16* (5), 6750–6756.
682 <https://doi.org/10.3892/mmr.2017.7444>.

- 683 (9) Zissimopoulos, S.; Seifan, S.; Maxwell, C.; Williams, A. J.; Lai, F. A. Disparities in the
684 Association of the Ryanodine Receptor and the FK506-Binding Proteins in Mammalian
685 Heart. *J. Cell Sci.* **2012**, *125* (7), 1759–1769. <https://doi.org/10.1242/jcs.098012>.
- 686 (10) Towbin, J. A.; Lorts, A.; Jefferies, J. L. Left Ventricular Non-Compaction
687 Cardiomyopathy. *Lancet* **2015**, *386* (9995), 813–825. [https://doi.org/10.1016/S0140-
688 6736\(14\)61282-4](https://doi.org/10.1016/S0140-6736(14)61282-4).
- 689 (11) Monti, M.; Orrù, S.; Pagnozzi, D.; Pucci, P. Functional Proteomics. *Clin. Chim. Acta*
690 **2005**, *357* (2), 140–150. <https://doi.org/10.1016/j.cccn.2005.03.019>.
- 691 (12) Wasik, A. A.; Schiller, H. B. Functional Proteomics of Cellular Mechanosensing
692 Mechanisms. *Seminars in Cell and Developmental Biology*. July 1, 2017, pp 118–128.
693 <https://doi.org/10.1016/j.semcdb.2017.06.019>.
- 694 (13) Tay, A. P.; Liang, A.; Wilkins, M. R.; Pang, C. N. I. Visualizing Post-Translational
695 Modifications in Protein Interaction Networks Using PTMOracle. *Curr. Protoc.*
696 *Bioinforma.* **2019**, *66* (1), e71. <https://doi.org/10.1002/cpbi.71>.
- 697 (14) Khymenets, O.; Joglar, J.; Clapés, P.; Parella, T.; Covas, M.-I.; de la Torre, R.
698 Biocatalyzed Synthesis and Structural Characterization of Monoglucuronides of
699 Hydroxytyrosol, Tyrosol, Homovanillic Alcohol, and 3-(4'-Hydroxyphenyl)Propanol.
700 *Adv. Synth. Catal.* **2006**, *348* (15), 2155–2162. <https://doi.org/10.1002/adsc.200606221>.
- 701 (15) Catalán, Ú.; López de las Hazas, M. C.; Piñol, C.; Rubió, L.; Motilva, M. J.; Fernandez-
702 Castillejo, S.; Solà, R. Hydroxytyrosol and Its Main Plasma Circulating Metabolites
703 Attenuate the Initial Steps of Atherosclerosis through Inhibition of the MAPK Pathway.
704 *J. Funct. Foods* **2018**, *40*, 280–291. <https://doi.org/10.1016/j.jff.2017.11.007>.
- 705 (16) Perez-Riverol, Y.; Csordas, A.; Bai, J.; Bernal-Llinares, M.; Hewapathirana, S.; Kundu,
706 D. J.; Inuganti, A.; Griss, J.; Mayer, G.; Eisenacher, M.; Erez, E. P.; Uszkoreit, J.;
707 Pfeuffer, J.; Sachsenberg, T.; Ule Yilmaz, S. ; Tiwary, S.; Urgen Cox, J. ; Audain, E.;

- 708 Walzer, M.; Jarnuczak, A. F.; Terner, T.; Brazma, A.; Vizcaíno, J. A. The PRIDE
709 Database and Related Tools and Resources in 2019: Improving Support for
710 Quantification Data. *Nucleic Acids Res.* **2019**, *47*. <https://doi.org/10.1093/nar/gky1106>.
- 711 (17) Method of the Year 2012. *Nat. Methods* **2013**, *10* (1), 1–1.
712 <https://doi.org/10.1038/nmeth.2329>.
- 713 (18) Aebersold, R.; Burlingame, A. L.; Bradshaw, R. A. Western Blots versus Selected
714 Reaction Monitoring Assays: Time to Turn the Tables? *Molecular and Cellular*
715 *Proteomics*. September 2013, pp 2381–2382. <https://doi.org/10.1074/mcp.E113.031658>.
- 716 (19) Castejón, M. L.; Montoya, T.; Alarcón-de-la-lastra, C.; Sánchez-hidalgo, M. Potential
717 Protective Role Exerted by Secoiridoids from *Olea Europaea* L. In Cancer,
718 Cardiovascular, Neurodegenerative, Aging-Related, and Immunoinflammatory Diseases.
719 *Antioxidants*. MDPI AG February 1, 2020. <https://doi.org/10.3390/antiox9020149>.
- 720 (20) Tomé-Carneiro, J.; Crespo, M. C.; García-Calvo, E.; Luque-García, J. L.; Dávalos, A.;
721 Visioli, F. Proteomic Evaluation of Mouse Adipose Tissue and Liver Following
722 Hydroxytyrosol Supplementation. *Food Chem. Toxicol.* **2017**, *107* (Pt A), 329–338.
723 <https://doi.org/10.1016/j.fct.2017.07.009>.
- 724 (21) Coumans, J. V. F.; Gau, D.; Poljak, A.; Wasinger, V.; Roy, P.; Moens, P. D. J. Profilin-1
725 Overexpression in MDA-MB-231 Breast Cancer Cells Is Associated with Alterations in
726 Proteomics Biomarkers of Cell Proliferation, Survival, and Motility as Revealed by
727 Global Proteomics Analyses. *Omi. A J. Integr. Biol.* **2014**, *18* (12), 778–791.
728 <https://doi.org/10.1089/omi.2014.0075>.
- 729 (22) Zhao, Q.; Wu, K.; Li, N.; Li, Z.; Jin, F. Identification of Potentially Relevant Genes for
730 Myocardial Infarction Using RNA Sequencing Data Analysis. *Exp. Ther. Med.* **2018**, *15*
731 (2), 1456–1464. <https://doi.org/10.3892/etm.2017.5580>.
- 732 (23) Rudel, L. L.; Lee, R. G.; Parini, P. ACAT2 Is a Target for Treatment of Coronary Heart

- 733 Disease Associated with Hypercholesterolemia. *Arteriosclerosis, Thrombosis, and*
734 *Vascular Biology*. June 1, 2005, pp 1112–1118.
735 <https://doi.org/10.1161/01.ATV.0000166548.65753.1e>.
- 736 (24) Denuc, A.; Núñez, E.; Calvo, E.; Loureiro, M.; Miro-Casas, E.; Guarás, A.; Vázquez, J.;
737 Garcia-Dorado, D. New Protein-Protein Interactions of Mitochondrial Connexin 43 in
738 Mouse Heart. *J. Cell. Mol. Med.* **2016**, *20* (5), 794–803.
739 <https://doi.org/10.1111/jcmm.12792>.
- 740 (25) Xu, Z. W.; Chen, X.; Jin, X. H.; Meng, X. Y.; Zhou, X.; Fan, F. X.; Mao, S. Y.; Wang,
741 Y.; Zhang, W. C.; Shan, N. N.; Li, Y. M.; Xu, R. C. SILAC-Based Proteomic Analysis
742 Reveals That Salidroside Antagonizes Cobalt Chloride-Induced Hypoxic Effects by
743 Restoring the Tricarboxylic Acid Cycle in Cardiomyocytes. *J. Proteomics* **2016**, *130*,
744 211–220. <https://doi.org/10.1016/j.jprot.2015.09.028>.
- 745 (26) Wiersma, M.; Meijering, R. A. M.; Qi, X. Y.; Zhang, D.; Liu, T.; Hoogstra-Berends, F.;
746 Sibon, O. C. M.; Henning, R. H.; Nattel, S.; Brundel, B. J. J. M. Endoplasmic Reticulum
747 Stress Is Associated with Autophagy and Cardiomyocyte Remodeling in Experimental
748 and Human Atrial Fibrillation. *J. Am. Heart Assoc.* **2017**, *6* (10), e006458.
749 <https://doi.org/10.1161/JAHA.117.006458>.
- 750 (27) Hwang, J. W.; Jang, M. A.; Jang, S. Y.; Seo, S. H.; Seong, M. W.; Park, S. S.; Ki, C. S.;
751 Kim, D. K. Diverse Phenotypic Expression of Cardiomyopathies in a Family with
752 TNNI3 p.Arg145Trp Mutation. *Korean Circ. J.* **2017**, *47* (2), 270–277.
753 <https://doi.org/10.4070/kcj.2016.0213>.
- 754 (28) Mao, C.; Howard, T. D.; Sullivan, D.; Fu, Z.; Yu, G.; Parker, S. J.; Will, R.; Vander
755 Heide, R. S.; Wang, Y.; Hixson, J.; Van Eyk, J.; Herrington, D. M. Bioinformatic
756 Analysis Of Coronary Disease Associated SNPs And Genes To Identify Proteins
757 Potentially Involved In The Pathogenesis Of Atherosclerosis. *J. Proteomics Genomics*
758 *Res.* **2017**, *2* (1), 1–12. <https://doi.org/10.14302/issn.2326-0793.jpgr-17-1447>.

- 759 (29) Liu, S.; JIAnG, H.; Wen, H.; Ding, Q.; Feng, C. C. Knockdown of Tyrosine 3-
760 Monooxygenase/Tryptophan 5-Monooxygenase Activation Protein Zeta (YWHAZ)
761 Enhances Tumorigenesis Both in Vivo and in Vitro in Bladder Cancer. *Oncol. Rep.*
762 **2018**, *39* (5), 2127–2135. <https://doi.org/10.3892/or.2018.6294>.
- 763 (30) Gęgotek, A.; Domingues, P.; Skrzydlewska, E. Proteins Involved in the Antioxidant and
764 Inflammatory Response in Rutin-Treated Human Skin Fibroblasts Exposed to UVA or
765 UVB Irradiation. *J. Dermatol. Sci.* **2018**, *90* (3), 241–252.
766 <https://doi.org/10.1016/j.jdermsci.2018.02.002>.
- 767 (31) Wang, W.; Zhang, L.; Wang, Y.; Ding, Y.; Chen, T.; Wang, Y.; Wang, H.; Li, Y.; Duan,
768 K.; Chen, S.; Yang, Q.; Chen, C. Involvement of MiR-451 in Resistance to Paclitaxel by
769 Regulating YWHAZ in Breast Cancer. *Cell Death Dis.* **2017**, *8* (10), e3071.
770 <https://doi.org/10.1038/cddis.2017.460>.
- 771 (32) Watanabe, N.; Komatsu, S.; Ichikawa, D.; Miyamae, M.; Ohashi, T.; Okajima, W.;
772 Kosuga, T.; Konishi, H.; Shiozaki, A.; Fujiwara, H.; Okamoto, K.; Tsuda, H.; Otsuji, E.
773 Overexpression of YWHAZ as an Independent Prognostic Factor in Adenocarcinoma of
774 the Esophago-Gastric Junction. *Am. J. Cancer Res.* **2016**, *6* (11), 2729–2736.
- 775 (33) Moraru, E.; Vilcea, I. D.; Mirea, C. S.; Mogoantă, S. Ş.; Cruce, M.; Vasile, I.; Vasile,
776 M.; Vilcea, A. M. C-Abl and YWHAZ Gene Expression in Gastric Cancer. *Rom. J.*
777 *Morphol. Embryol.* **2015**, *56* (2 Suppl), 717–723.
- 778 (34) Li, T.; Wang, Y.; Gao, Y.; Li, Q. Identification and Characterisation of the Anti-
779 Oxidative Stress Properties of the Lamprey Prohibitin 2 Gene. *Fish Shellfish Immunol.*
780 **2015**, *42* (2), 447–456. <https://doi.org/10.1016/j.fsi.2014.11.016>.
- 781 (35) Xu, J.; Bian, X.; Liu, Y.; Hong, L.; Teng, T.; Sun, Y.; Xu, Z. Adenosine A2 Receptor
782 Activation Ameliorates Mitochondrial Oxidative Stress upon Reperfusion through the
783 Posttranslational Modification of NDUFV2 Subunit of Complex I in the Heart. *Free*

- 784 *Radic. Biol. Med.* **2017**, *106*, 208–218.
785 <https://doi.org/10.1016/j.freeradbiomed.2017.02.036>.
- 786 (36) Bećarević, M. TNF-Alpha and Annexin A2: Inflammation in Thrombotic Primary
787 Antiphospholipid Syndrome. *Rheumatology International*. December 4, 2016, pp 1649–
788 1656. <https://doi.org/10.1007/s00296-016-3569-1>.
- 789 (37) Fairwozy, R. H.; Cooper, J.; White, J.; Giambartolomei, C.; Folkersen, L.; Wannamethee,
790 S. G.; Jefferis, B. J.; Whincup, P.; Ben-Shlomo, Y.; Kumari, M.; Kivimaki, M.; Wong,
791 A.; Hardy, R.; Kuh, D.; Gaunt, T. R.; Casas, J. P.; McLachlan, S.; Price, J. F.; Hingorani,
792 A.; Franco-Cereceda, A.; Grewal, T.; Kalea, A. Z.; Humphries, S. E. Identifying Low
793 Density Lipoprotein Cholesterol Associated Variants in the Annexin A2 (ANXA2)
794 Gene. *Atherosclerosis* **2017**, *261*, 60–68.
795 <https://doi.org/10.1016/j.atherosclerosis.2017.04.010>.
- 796 (38) Brown, A. M.; Gordon, D.; Lee, H.; Vrièze, F. W. De; Cellini, E.; Bagnoli, S.; Nacmias,
797 B.; Sorbi, S.; Hardy, J.; Blass, J. P. Testing for Linkage and Association across the
798 Dihydrolipoyl Dehydrogenase Gene Region with Alzheimer’s Disease in Three Sample
799 Populations. *Neurochem. Res.* **2007**, *32* (4–5), 857–869. [https://doi.org/10.1007/s11064-](https://doi.org/10.1007/s11064-006-9235-3)
800 [006-9235-3](https://doi.org/10.1007/s11064-006-9235-3).
- 801 (39) Morton, N. M.; Nelson, Y. B.; Michailidou, Z.; Rollo, E. M.; Ramage, L.; Hadoke, P. W.
802 F.; Seckl, J. R.; Bunger, L.; Horvat, S.; Kenyon, C. J.; Dunbar, D. R. A Stratified
803 Transcriptomics Analysis of Polygenic Fat and Lean Mouse Adipose Tissues Identifies
804 Novel Candidate Obesity Genes. *PLoS One* **2011**, *6* (9), e23944.
805 <https://doi.org/10.1371/journal.pone.0023944>.
- 806 (40) Zhou, N.; Stoll, S.; Qiu, H. VCP Represses Pathological Cardiac Hypertrophy. *Aging*.
807 December 26, 2017, pp 2469–2470. <https://doi.org/10.18632/aging.101357>.
- 808 (41) Lizano, P.; Rashed, E.; Kang, H.; Dai, H.; Sui, X.; Yan, L.; Qiu, H.; Depre, C. The

- 809 Valosin-Containing Protein Promotes Cardiac Survival through the Inducible Isoform of
810 Nitric Oxide Synthase. *Cardiovasc. Res.* **2013**, *99* (4), 685–693.
811 <https://doi.org/10.1093/cvr/cvt136>.
- 812 (42) Feng, L.; Ma, X.; Wang, J.; Tian, Q. Up-Regulation of 14-3-3 β Plays a Role in Intimal
813 Hyperplasia Following Carotid Artery Injury in Diabetic Sprague Dawley Rats by
814 Promoting Endothelial Cell Migration and Proliferation. *Biochem. Biophys. Res.*
815 *Commun.* **2017**, *490* (4), 1237–1243. <https://doi.org/10.1016/j.bbrc.2017.06.199>.
- 816 (43) Frasinuk, M. S.; Zhang, W.; Wyrebek, P.; Yu, T.; Xu, X.; Sviripa, V. M.; Bondarenko,
817 S. P.; Xie, Y.; Ngo, H. X.; Morris, A. J.; Mohler, J. L.; Fiandalo, M. V.; Watt, D. S.; Liu,
818 C. Developing Antineoplastic Agents That Target Peroxisomal Enzymes: Cytisine-
819 Linked Isoflavonoids as Inhibitors of Hydroxysteroid 17-Beta-Dehydrogenase-4
820 (HSD17B4). *Org. Biomol. Chem.* **2017**, *15* (36), 7623–7629.
821 <https://doi.org/10.1039/c7ob01584d>.
- 822 (44) Christians, E. S.; Ishiwata, T.; Benjamin, I. J. Small Heat Shock Proteins in Redox
823 Metabolism: Implications for Cardiovascular Diseases. *Int. J. Biochem. Cell Biol.* **2012**,
824 *44* (10), 1632–1645. <https://doi.org/10.1016/j.biocel.2012.06.006>.
- 825 (45) Deniset, J. F.; Hedley, T. E.; Hlaváčková, M.; Chahine, M. N.; Dibrov, E.; O’Hara, K.;
826 Maddaford, G. G.; Nelson, D.; Maddaford, T. G.; Fandrich, R.; Kardami, E.; Pierce, G.
827 N. Heat Shock Protein 60 Involvement in Vascular Smooth Muscle Cell Proliferation.
828 *Cell. Signal.* **2018**, *47*, 44–51. <https://doi.org/10.1016/j.cellsig.2018.03.011>.
- 829 (46) Kanellos, G.; Frame, M. C. Cellular Functions of the ADF/Cofilin Family at a Glance. *J.*
830 *Cell Sci.* **2016**, *129* (17), 3211–3218. <https://doi.org/10.1242/jcs.187849>.
- 831 (47) Wang, Q. zhen; Gao, H. qing; Liang, Y.; Zhang, J.; Wang, J.; Qiu, J. Cofilin1 Is
832 Involved in Hypertension-Induced Renal Damage via the Regulation of NF-KB in Renal
833 Tubular Epithelial Cells. *J. Transl. Med.* **2015**, *13* (1), 323.

- 834 <https://doi.org/10.1186/s12967-015-0685-8>.
- 835 (48) Hosseini, M.; Najmabadi, H.; Kahrizi, K. Calpains: Diverse Functions but Enigmatic.
836 *Arch. Iran. Med.* **2018**, *21* (4), 170–179.
- 837 (49) Muniappan, L.; Javidan, A.; Jiang, W.; Mohammadmoradi, S.; Moorlegghen, J. J.; Katz,
838 W. S.; Balakrishnan, A.; Howatt, D. A.; Subramanian, V. Calpain Inhibition Attenuates
839 Adipose Tissue Inflammation and Fibrosis in Diet-Induced Obese Mice. *Sci. Rep.* **2017**,
840 *7* (1), 14398. <https://doi.org/10.1038/s41598-017-14719-9>.
- 841 (50) Mann, M.; Jensen, O. N. Proteomic Analysis of Post-Translational Modifications. *Nat.*
842 *Biotechnol.* **2003**, *21* (3), 255–261. <https://doi.org/10.1038/nbt0303-255>.
- 843 (51) Chen, H.; Zhang, W.; Sun, X.; Yoshimoto, M.; Chen, Z.; Zhu, W.; Liu, J.; Shen, Y.;
844 Yong, W.; Li, D.; Zhang, J.; Lin, Y.; Li, B.; VanDusen, N. J.; Snider, P.; Schwartz, R. J.;
845 Conway, S. J.; Field, L. J.; Yoder, M. C.; Firulli, A. B.; Carlesso, N.; Towbin, J. A.;
846 Shou, W. Fkbp1a Controls Ventricular Myocardium Trabeculation and Compaction by
847 Regulating Endocardial Notch1 Activity. *Dev.* **2013**, *140* (9), 1946–1957.
848 <https://doi.org/10.1242/dev.089920>.
- 849 (52) Fei, J.; Sun, Y.; Duan, Y.; Xia, J.; Yu, S.; Ouyang, P.; Wang, T.; Zhang, G. Low
850 Concentration of Rutin Treatment Might Alleviate the Cardiotoxicity Effect of
851 Pirarubicin on Cardiomyocytes via Activation of PI3K/AKT/MTOR Signaling Pathway.
852 *Biosci. Rep.* **2019**, *39* (6), BSR20190546. <https://doi.org/10.1042/BSR20190546>.
- 853 (53) Nakaoka, Y.; Nishida, K.; Narimatsu, M.; Kamiya, A.; Minami, T.; Sawa, H.; Okawa,
854 K.; Fujio, Y.; Koyama, T.; Maeda, M.; Sone, M.; Yamasaki, S.; Arai, Y.; Gou, Y. K.;
855 Kodama, T.; Hirota, H.; Otsu, K.; Hirano, T.; Mochizuki, N. Gab Family Proteins Are
856 Essential for Postnatal Maintenance of Cardiac Function via Neuregulin-1/ErbB
857 Signaling. *J. Clin. Invest.* **2007**, *117* (7), 1771–1781. <https://doi.org/10.1172/JCI30651>.
- 858 (54) Kajiwara, Y.; Wang, E.; Wang, M.; Sin, W. C.; Brennand, K. J.; Schadt, E.; Naus, C. C.;

859 Buxbaum, J.; Zhang, B. GJA1 (Connexin43) Is a Key Regulator of Alzheimer's Disease
860 Pathogenesis. *Acta Neuropathol. Commun.* **2018**, 6 (1), 144.
861 <https://doi.org/10.1186/s40478-018-0642-x>.

862 **FUNDING SOURCES**

863 The work summarized in this manuscript was supported in part by grants (Grant Nos. MEFOPC
864 Project, AGL2012-40144-C03-02 and AGL2012-40144-C03-03, and AppleCOR Project,
865 AGL2016-76943-C2-2-R) from the Ministerio de Economía, Industria y Competitividad, the
866 Agencia Estatal de Investigación (AEI), and the European Regional Development Fund
867 (ERDF). L. Rubió enjoys a Sara Borrell post-doctoral grant (CD14/00275; Spain), A. Pedret
868 enjoys a post-doctoral grant (PTQ-15-08068; Spain), and Ú. Catalán enjoys a Pla estratègic de
869 recerca i innovació en salut (PERIS) post-doctoral grant (SLT002/16/00239; Catalunya, Spain).

870

871

872

873

874

875

876

877

878

879

880

881

882 **FIGURE CAPTIONS**

883 **Figure 1. PPIs to FKBP1A in Heart Cardiovascular System Network after SEC**

884 **supplemented diets.** PPIs differentially expressed in the heart tissue after the SEC diet and
885 other important proteins related to the same network. Proteins are represented in red or green
886 color if the protein is up- or downregulated, respectively.

887 **Figure 2. PPIs to GJA1 in Aorta Cardiovascular System Network SEC supplemented**

888 **diets.** PPIs differentially expressed in the aorta tissue after the SEC diet and other important
889 proteins related to the same network. Proteins are represented in red or green color if the protein
890 is up- or downregulated, respectively.

891 **Figure 3. The integrated network between heart PPIs and its phosphoproteome analysis.**

892 Interaction between the PPIs differentially expressed in the heart after the SEC diet and the
893 phosphorylated or dephosphorylated proteins, and other important proteins related to the same
894 network. Proteins are represented in red or green color if the protein is up- or downregulated,
895 respectively.

896

897

Table 1. Biochemical Parameters in Female Wistar Rat Plasma After the Experiment.

Biochemical parameters	Control group (n=4)	Secoiridoid group (n=4)	<i>p</i> between groups
	Mean (SD)	Mean (SD)	
Glucose (mg/dL)	198.75 (2.75)	204.25 (18.46)	0.595
Insulin (µg/L)	0.608 (0.06)	1.768 (0.91)	0.103
Total Cholesterol (mg/dL)	72.39 (10.65)	66.02 (8.79)	0.392
Triglycerides (mg/dL)	51.10 (30.13)	54.39 (18.62)	0.859
HDL cholesterol (mg/dL)	60.94 (10.31)	56.17 (5.11)	0.438
Non-HDL cholesterol (mg/dL)	11.45 (1.70)	9.85 (4.98)	0.568

HDL, high-density lipoprotein; SD, standard deviation

Unpaired student t-test was used for analysis between two groups. A value of $p < 0.05$ was considered statistically significant.

Table 2. Heart Significant Proteins From the Unpaired Student's t-test Between SEC and Control Group that Interacts to FKBP1A.

UniProt ID	Gene Symbol	Protein name	MW (kDa)	<i>p</i>	FC (SEC <i>versus</i> control group)
P23693	Tnni3	Troponin I, cardiac muscle	24.10	0.032*	2.43
P17764	Acat1	Acetyl-CoA acetyltransferase, mitochondrial	44.70	0.029*	4.52
P06761	Hspa5	78 kDa glucose-regulated protein	72.30	0.021*	1.57
P27605	Hprt1	Hypoxanthine-guanine phosphoribosyltransferase	24.50	0.011*	2.74
P35745	Acyp2	Acylphosphatase-2	10.90	<0.001*	2.58
P15865	Hist1h1d	Histone H1.4	22.00	<0.001*	2.37
P11608	ATP8	ATP synthase protein 8	7.60	<0.001*	1.20
P13086	Suclg1	Succinate--CoA ligase [ADP/GDP-forming] subunit alpha, mitochondrial	36.10	<0.001*	1.31
P63102	Ywhaz	14-3-3 protein zeta/delta	27.80	<0.001*	1.64
Q5XIH7	Phb2	Prohibitin-2	33.30	<0.001*	1.66
P20759	Ighg1	Ig gamma-1 chain C region	35.90	0.011*	-1.83
P26772	Hspe1	10 kDa heat shock protein, mitochondrial	10.90	<0.001*	-1.61
P36201	Crip2	Cysteine-rich protein 2	22.70	<0.001*	-2.13

MW, molecular weight; FC, fold change, and SEC, secoiridoids.

*A value of $p < 0.05$ was considered statistically significant.

Table 3. Aorta Significant Proteins From the Unpaired Student's t-test Between SEC and Control Group that Interacts to GJA1.

UniProt ID	Gene symbol	Protein name	MW (kDa)	<i>p</i>	FC (SEC versus control group)
P19234	Ndufv2	NADH dehydrogenase [ubiquinone] flavoprotein 2. mitochondrial	27.40	<0.001*	1.41
P01835	Igkc	Ig kappa chain C region. B allele	11.60	<0.001*	1.64
P20767	N/A	Ig lambda-2 chain C region	11.30	0.012*	1.72
P20761	Igh-1a	Ig gamma-2B chain C region	36.50	0.022*	2.13
Q8VIF7	Selenbp1	Selenium-binding protein 1	52.50	0.033*	1.72
P01805	N/A	Ig heavy chain V region IR2	16.00	0.037*	2.33
P52555	Erp29	Endoplasmic reticulum resident protein 29	28.60	<0.001*	-1.48
Q6P6R2	Dld	Dihydrolipoyl dehydrogenase. mitochondrial	54.00	<0.001*	-16.00
Q64537	Capns1	Calpain small subunit 1	28.60	<0.001*	-1.17
P61206	Arf3	ADP-ribosylation factor 3	20.60	<0.001*	-16.00
P68370	Tuba1a	Tubulin alpha-1A chain	50.10	<0.001*	-3.43
Q6P9V9	Tuba1b	Tubulin alpha-1B chain	50.10	<0.001*	-3.77
P46462	Vcp	Transitional endoplasmic reticulum ATPase	89.30	0.002*	-4.05
P68255	Ywhaq	14-3-3 protein theta	27.80	0.002*	-1.96
P97852	Hsd17b4	Peroxisomal multifunctional enzyme type 2	79.40	0.004*	-1.96
P35213	Ywhab	14-3-3 protein beta/alpha	28.00	0.004*	-2.07
Q07936	Anxa2	Annexin A2	38.70	0.012*	-2.19
P48675	Des	Desmin	53.40	0.013*	-2.11
Q08290	Cnn1	Calponin-1	33.30	0.013*	-2.54
P63102	Ywhaz	14-3-3 protein zeta/delta	27.80	0.014*	-2.40
Q9QXQ0	Actn4	Alpha-actinin-4	104.80	0.024*	-2.00
P42930	Hspb1	Heat shock protein beta-1	22.90	0.025*	-3.30
P62271	Rps18	40S ribosomal protein S18	17.70	0.029*	-2.02
P62828	Ran	GTP-binding nuclear protein Ran	24.40	0.034*	-3.20
P01946	Hba1	Hemoglobin subunit alpha-1/2	15.30	0.044*	-1.76
Q7M0E3	Dstn	Destrin	18.50	0.048*	-2.68
P45592	Cfl1	Cofilin-1	18.50	0.049*	-2.23

MW. molecular weight; FC. fold change. and SEC. secoiridoids.

*A value of $p < 0.05$ was considered statistically significant.

Table 4. Relevant Diseases and Biological Functions of the Proteins Involved in the Cardiovascular Disease Network From Heart or Aorta Tissues Predicted by the Ingenuity Pathway Analysis Software.

Diseases and Functions	Tissue	
	Heart	Aorta
Cardiovascular disease	KCNJ11, SUCLG1 , IDH2, HSPE1 , ERN1, TNNI3 , FKBP1A , P38 MAPK, MYC, CRYAB, and GATA4	KCNJ11, Tpm1, IGF1R, TJP1, CACNA1A, CACNA1B, GJA1 , PRKCA, calpain , TUBA1A , MAPK14, NOS2, TSC2, HSPB1 , CRYAB, E2F1, and CTNNB1
Cardiovascular System Development and Function	KCNJ11, RAB10, IDH2, ERN1, YWHAZ , P38 MAPK, HSPA5 , TNNI3 , FKBP1A , MYC, CRYAB, and GATA4	KCKNJ11, Tpm1, CLIC4, ANXA2 , IGF1R, CDH1, TJP1, CACNA1B, GJA1 , PRKCA, NDUFV2 , Mapk, TSC2, NOS2, MAPK14, YWHAZ , HSPB1 , CRYAB, E2F1, and CTNNB1
Metabolic Disease	SLC1A2, TFRC, KCNJ11, ACAT1 , SUCLG1 , YWHAZ , ERN1, 26s Proteasome, IDH2, HSPA5 , TNNI3 , FKBP1A , and MYC	KCKNJ11, ANXA2 , IGF1R, CACNA1A, CACNA1B, PRKCA, TUBA1A , MAPK14, NOS2, TSC2, HSPB1 , HSD17B4 , BAD, E2F1, and CTNNB1
Lipid Metabolism	SUCLG1 , ACAT1 , FKBP1A , HSPA5 , and MYC	-
Inflammatory disease	SLC1A2, TFRC, PHB2 , RAB10, MYO1C, ERN1, 26s Proteasome, HSPE1 , HSPA5 , TNNI3 , FKBP1A , and CRYAB	IGF1R, CDH1, TJP1, CACNA1A, CACNA1B, PRKCA, Calpain , TUBA1A , MAPK14, NOS2, 26s Proteasome, BAD, CRYAB, and CTNNB1
Inflammatory response	SLC1A2, TFRC, PHB2 , RAB10, MYO1C, ERN1, 26s Proteasome, HSPA5 , TNNI3 , FKBP1A , and CRYAB	ANXA2 , IGF1R, CDH1, GJA1 , MAPK14, NOS2, and 26s Proteasome
Cancer	SLC1A2, TFRC, KCNJ11, SUCLG1 , ACAT1 , RAB10, IDH2, MYO1C, Hsp90, ERN1, YWHAZ , 26s Proteasome, FKBP1A , HSPA5 , MYC, CRYAB, and GATA4	KCKNJ11, Tpm1, CLIC4, ANXA2 , IGF1R, CDH1, TJP1, CACNA1A, CACNA1B, GJA1 , PRKCA, HGS, TUBA1A , MAPK14, NOS2, TSC2, HSPB1 , Mapk, NDUFV2 , DLD , HSD17B4 , VCP , 26s Proteasome, YWHAZ , BAD, YWHAB , CRYAB, E2F1, CTNNB1, RAN , and CFL1
Free Radical Scavenging	-	ANXA2 , PRKCA, Calpain , Mapk, YWHAZ , MAPK14, NOS2, TSC2, HSPB1 , CRYAB, and E2F1
Neurological disease	SLC1A2, TFRC, KCNJ11, SUCLG1 , ACAT1 , PHB2 , YWHAZ , HSPA5 , FKBP1A , IDH2, MYC, CRYAB, and GATA4	KCKNJ11, ANXA2 , IGF1R, CDH1, TJP1, CACNA1A, CACNA1B, GJA1 , PRKCA, Calpain , TUBA1A , MAPK14, NOS2, TSC2, CHMP2B, HSPB1 , Mapk, NDUFV2 , HSD17B4 , VCP , 26s Proteasome, YWHAZ , BAD, YWHAB , CRYAB, E2F1, CTNNB1, and RAN
Immunological disease	MYC, CRYAB, IDH2, Hsp90, YWHAZ , 26s Proteasome, TFRC, and FKBP1A	Tpm1, ANXA2 , CH1, TJP1, GJA1 , PRKCA, VCP , 26s Proteasome, YWHAZ , BAD, TUBA1A , NOS2, TSC2, HSPB1 , CRYAB, E2F1, CTNNB1, RAN , and CFL1
Gastrointestinal disease	SLC1A2, TFRC, KCNJ11, SUCLG1 , ACAT1 , YWHAZ , RAB10, IDH2, MYO1C, FKBP1A , Hsp90, ERN1, HSPA5 , and MYC	KCNJ11, CLIC4, ANXA2 , IGF1R, CDH1, TJP1, CACNA1B, GJA1 , CACNA1A, VCP , HSD17B4 , DLD , YWHAZ , BAD, MAPK14, TUBA1A , NOS2, HGS, PRKCA, HSPB1 , TSC2, Mapk, NDUFV2 , E2F1, RAN , and CTNNB1
Hepatic system disease	SLC1A2, TFRC, KCNJ11, SUCLG1 , ACAT1 , YWHAZ , IDH2, RAB10, MYO1C, FKBP1A , Hsp90, ERN1, HSPA5 , and MYC	KCNJ11, CLIC4, ANXA2 , IGF1R, CDH1, TJP1, CACNA1B, GJA1 , CACNA1A, VCP , HSD17B4 , DLD , YWHAZ , BAD, MAPK14, NOS2, TUBA1A , HGS, HSPB1 , TSC2, Mapk, NDUFV2 , E2F1, RAN , and CTNNB1

Proteins marked in **bold** are significant proteins with physical protein-protein interaction to FKBP1A (heart) or to GJA1 (aorta) found in the SEC group compared to control group.

Proteins marked no-bold are other proteins not found in our study but which are predicted to be involved in the same network.

Table 5. Significant Phosphorylated Proteins After the Phospho-proteomic Analysis of Heart Tissue.

Peptide sequence	UniProt ID	Gene	Protein name	Molecular Function	Biological process	MW (kDa)	P	Phosphorylation FC (SEC versus control group)	Serine phosphorylation site
TRTFSATVR	Q9WU49	Carhsp1	Calcium-regulated heat stable protein 1	mRNA 3'-UTR binding	calcium-mediated signaling regulation of mRNA stability	1.12	0.0234	556.51	S5
RLSPSASPPR	B2RYB3	Srrm1	Serine and arginine repetitive matrix 1	nr	mRNA processing	1.23	0.0243	248.80	S3; S7
QRRESGEGEEEVADSAR	F1LT49	Lrrc47	Leucine-rich repeat-containing 47	phenylalanine-tRNA ligase activity RNA binding	nr	1.98	0.0226	201.67	S5
ASSCETYEYPTR	F1LSR2	Gab2	GRB2-associated-binding protein 2	transmembrane receptor protein tyrosine kinase adaptor activity	osteoclast differentiation positive regulation of cell population proliferation PI3K/mTOR signaling	1.54	0.0242	193.58	S3
LATTVSAPDLK	Q5M7W5	Map4	Microtubule-associated protein 4	microtubule binding	microtubule cytoskeleton organization neuron projection development	1.20	0.0244	111.80	S6
TSLSSLR	Q2PS20	Jph2	Junctophilin-2	calcium-release channel activity core promoter binding DNA binding phosphatidic acid binding phosphatidylinositol binding phosphatidylserine binding	multicellular organism development negative regulation of transcription, DNA-templated positive regulation of ryanodine-sensitive calcium-release channel activity regulation of cardiac muscle tissue development	0.84	0.0251	43.72	S2
TASAGTVSDAEVR	D4ADX8	Raph1	Ras association (RalGDS/AF-6) and pleckstrin homology domains 1	nr	axon extension signal transduction	1.34	0.0401	1.68	S3
NDSWGSFDLR	D3ZC82	Nufip2	Nuclear FMR1-interacting protein 2	RNA binding	nr	1.28	0.0237	1.66	S3
LPSPTVAR	F1M155	Svil	Supervillin	actin filament binding	cytoskeleton organization skeletal muscle tissue development	0.92	0.0234	1.57	S3

TGSLDESLSR	F1M6Z4	Prob1	Uncharacterized protein	nr	nr	1.14	0.0211	1.54	S3
TTSISPALAR	D3ZZQ0	Tnik	Similar to Traf2 and NCK interacting kinase, splice variant 4 (Predicted), isoform CRA_a	ATP binding protein serine/threonine kinase activity	activation of protein kinase activity MAPK cascade neuron projection morphogenesis signal transduction by protein phosphorylation stress-activated protein kinase signaling cascade	1.10	0.0058	1.53	S5
HGESAWNLENR	P25113	Pgam1	Phosphoglycerate mutase 1	nr	nr	1.39	0.0286	8.70	S4
	M0R9L0	Naca	Nascent polypeptide-associated complex subunit alpha	nr	nr	1.49	0.0286	16.71	S9
DAPTTLAESPSPK	P62804	Hist1h4b	Histone H4	DNA binding protein domain specific binding protein heterodimerization activity	cell differentiation DNA nucleosome assembly multicellular organism development negative regulation of megakaryocyte differentiation ossification protein heterotetramerization	1.42	0.0286	6.81	S3
RISGLIYEETR	Q5M7V8	Thrap3	Thyroid hormone receptor-associated protein 3	ATP binding nuclear receptor transcription coactivator activity phosphoprotein binding DNA binding thyroid hormone receptor binding transcription coactivator activity	circadian rhythm mRNA processing and stabilization catabolic process positive regulation of circadian rhythm splicing, via spliceosome RNA splicing	1.01	0.0410	1.36	S7
ASVSDLSPR STSPPPSPEVWAESR	D4A559	Dmtn	Dematin actin-binding protein	actin filament binding	actin filament bundle assembly lamellipodium assembly	1.71	0.0241	-121.78	S1
KKEPAISSQNSPEAR	Q4KLL0	Tcea1	Transcription elongation factor A protein 1	DNA binding zinc ion binding	positive regulation of exoribonuclease activity transcription, DNA-templated	1.72	0.0246	-251.45	S11
SKSPPKVPIVIQDDSLPT GPPPQIR	Q5XIA2	Szrd1	SUZ domain-containing protein 1	nr	nr	2.75	0.0265	-264.68	S3

ELALSSPEDLTQDFEELK R	P34926	Map1a	Microtubule-associated protein 1A	actin binding collagen binding microtubule binding tubulin binding	axonogenesis dendrite development microtubule cytoskeleton organization negative regulation of microtubule depolymerization regulation of microtubule depolymerization	2.38	0.0244	-293.42	S5; S6
QLHGHHKPNSEDLGDSA ESHFPR	G3V8S6	Hrc	Histidine rich calcium binding protein, isoform CRA_b	calcium ion binding	negative regulation of calcium ion import into sarcoplasmic reticulum	2.68	0.0258	-345.13	S16
DPGAVSPEPGKDHAQ PGR	E9PT87	Mylk3	Myosin light chain kinase 3	ATP binding calmodulin-dependent protein kinase activity myosin light chain kinase activity	cardiac myofibril assembly cellular response to interleukin-1 protein phosphorylation regulation of vascular permeability involved in acute inflammatory response sarcomere organization sarcomerogenesis	2.02	0.0216	-351.10	S6
GATPAEDDEDNDIDLF SDEEEDKEAAR	Q68FR9	Eef1d	Elongation factor 1-delta	DNA binding guanyl-nucleotide exchange factor activity translation elongation factor activity	cellular response to ionizing radiation translational elongation	3.26	0.0325	-435.53	S18
LQVPGGDSDEESKTPSA SPR	A0A0G2JUP3	Obscn	Obscurin, cytoskeletal calmodulin and titin- interacting RhoGEF	Rho guanyl-nucleotide exchange factor activity	regulation of Rho protein signal transduction	2.14	0.0245	-533.36	S8
RPPAMDDLDDSDN	M0R7Z4	Ptges3l	Prostaglandin E synthase 3-like	chaperone binding Hsp90 protein binding	chaperone-mediated protein complex assembly protein folding	1.75	0.0335	-538.53	S13

LLKEGEEPTVYSDDEEP KDEAAR	P70580	Pgrmc1	Membrane-associated progesterone receptor component 1	heme binding steroid binding	axon guidance memory modification of synaptic structure negative regulation of synapse organization positive regulation of protein localization to plasma membrane	2.70	0.0240	-801.76	S12
TPEELDDSDFETEDFDVR	A0A0G2JYF7	Ctnna1	Catenin alpha 1	actin filament binding beta-catenin binding cadherin binding structural molecule activity	actin filament organization aging axon regeneration epithelial cell-cell adhesion gap junction assembly male gonad development odontogenesis of dentin-containing tooth	2.24	0.0241	-819.04	S8
TEARSSDEENGPPSSPDL DR	D3ZH75	Akt1s1	AKT1 substrate 1	nr	negative regulation of cell size, protein kinase activity, and TOR signaling neurotrophin TRK receptor signaling pathway	2.32	<0.001	-2684.45	S5; S15
TREQESSGEEDNDLSPEE REK	A0A0H2UHA0	Ppp1r2	Protein phosphatase inhibitor 2	protein phosphatase inhibitor activity	regulation of signal transduction	2.54	<0.001	-5053.80	S7
DRSPSPLRGNVVPSPPLPT R	Q9WU49	Carhsp1	Calcium-regulated heat stable protein 1	mRNA 3'-UTR binding	calcium-mediated signaling regulation of mRNA stability	2.21	<0.001	-5747.82	S3; S5
SKSESPKEPEQLR	D4ACJ7	N/A	Uncharacterized protein	mRNA binding RNA binding	nr	1.64	<0.001	-2615.73	S3; S5

P08050	Gja1	Gap junction alpha-1 protein	<ul style="list-style-type: none"> beta-tubulin binding connexin binding disordered domain specific binding gap junction channel activity PDZ domain binding protein domain specific binding protein tyrosine kinase binding scaffold protein binding SH3 domain binding signaling receptor binding tubulin binding 	<ul style="list-style-type: none"> heart development apoptotic process ATP transport atrial ventricular junction remodeling blood vessel morphogenesis bone development and remodeling cardiac conduction cell-cell signaling cell communication chronic inflammatory endothelium development epithelial cell maturation gap junction assembly microtubule-based transport negative regulation of cardiac muscle cell proliferation, growth, cell population proliferation, DNA biosynthetic process, endothelial cell proliferation, gene expression, and wound healing neuron migration osteoblast differentiation positive regulation of behavioral fear response, blood vessel diameter, communication by chemical coupling, cold-induced thermogenesis, cytosolic calcium ion concentration, gene expression, glomerular filtration, insulin secretion, osteoblast differentiation, protein catabolic process, striated muscle tissue development, and vasoconstriction regulation of apoptotic process, atrial cardiac muscle cell membrane depolarization, bicellular tight junction assembly, bone mineralization and remodeling, calcium ion transport, transmembrane transporter activity, ventricular cardiac muscle cell membrane depolarization and repolarization response to estradiol, fluid shear stress, glucose, ischemia, lipopolysaccharide, peptide hormone, pH, and retinoic acid signal transduction skeletal muscle tissue regeneration T cell proliferation transmembrane transport vascular transport 	1.98	0.0294	-92.99	S3
--------	------	------------------------------	--	---	------	--------	--------	----

QASEQNWANYSAEQNR

M0R7R2	LOC683897	Similar to Protein C6orf203	nr	nr	2.54	0.0294	-119.84	S12
KTVQKDADEEDSDEETS								
HLER								

MW, molecular weight; FC, fold change, and SEC, secoiridoids; nr, not reported
Molecular function and Biological process source: UniProt (<https://www.uniprot.org/>).
*A value of $p < 0.05$ was considered statistically significant.

Figure 1

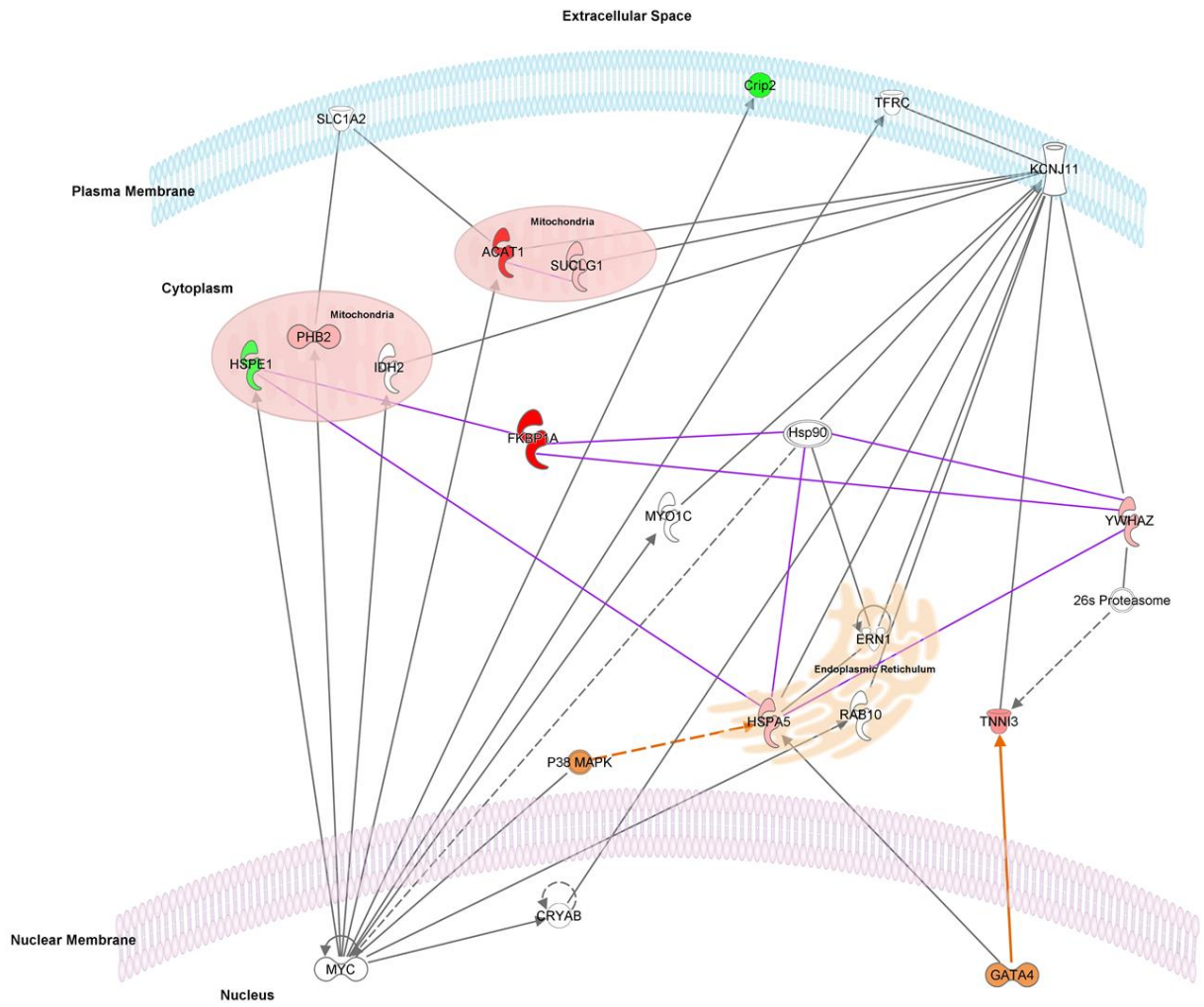


Figure 2

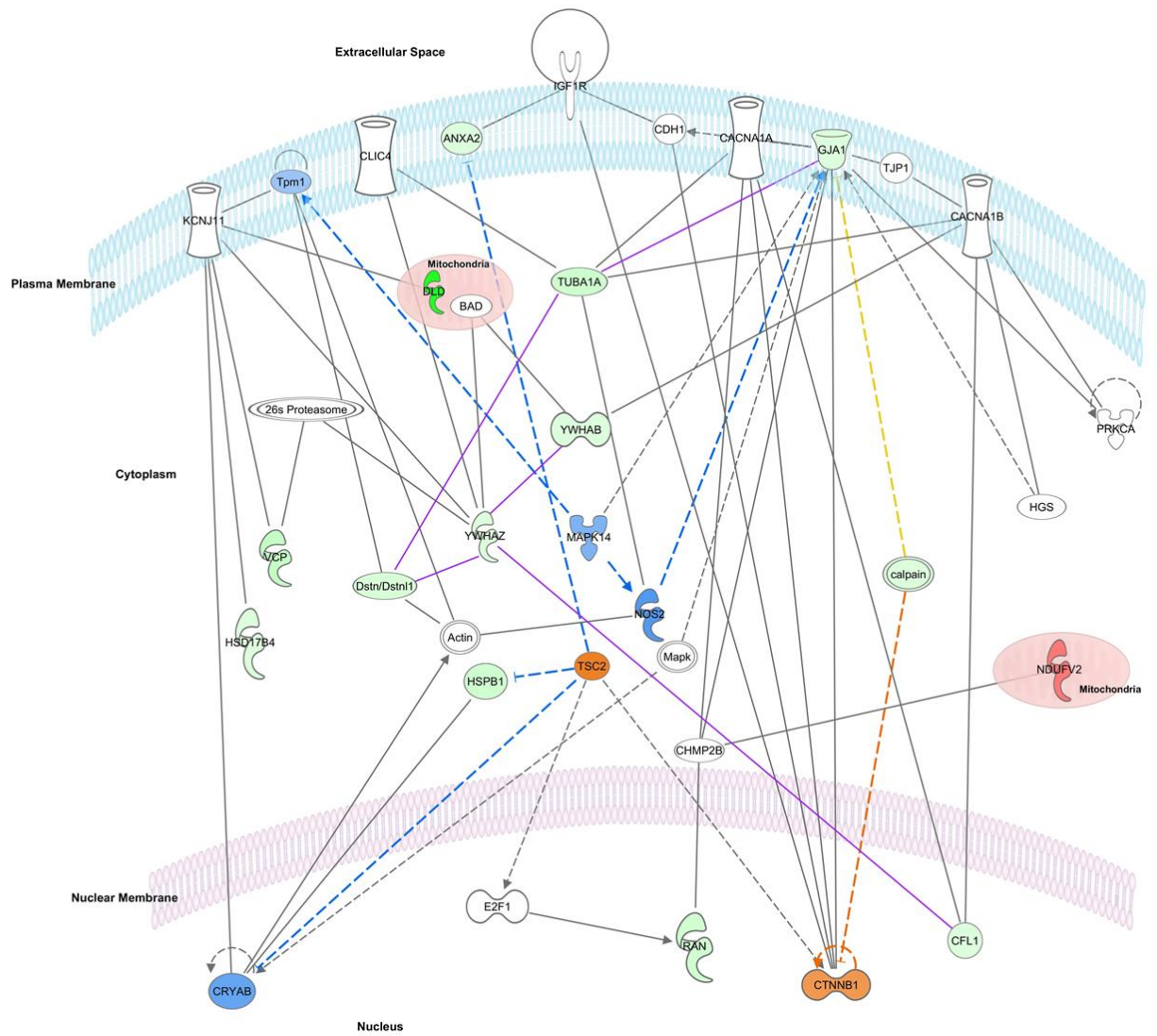
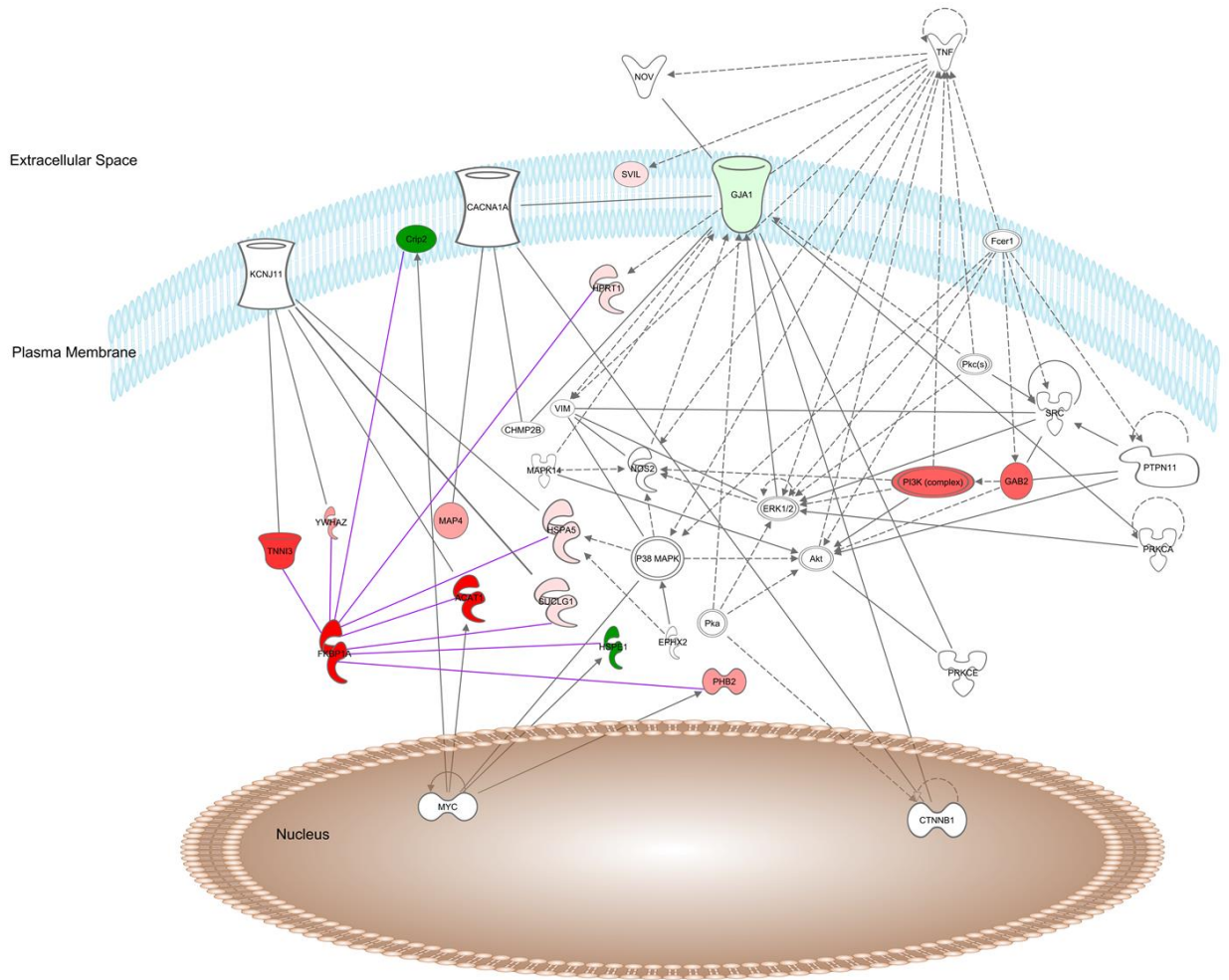


Figure 3



GRAPHIC FOR TABLE OF CONTENTS

